Digital Comprehensive Summaries of Uppsala Dissertations
from the Faculty of Science and Technology 2414

Invariant domain preserving schemes for magnetohydrodynamics

TUAN ANH DAO

ACTA UNIVERSITATIS
UPSALIENSIS
2024

ISSN 1651-6214
ISBN 978-91-513-2165-3
urn:nbn:se:uu:diva-532130

UPPSALA
UNIVERSITET

Dissertation presented at Uppsala University to be publicly examined in Sonja Lyttkens, 101121, Ångström, Lägerhyddsvägen 1, Uppsala, Friday, 6 September 2024 at 10:15 for the degree of Doctor of Philosophy. The examination will be conducted in English. Faculty examiner: Professor Remi Abgrall (Institute of Mathematics, University of Zürich).

Abstract
Dao, T. A. 2024. Invariant domain preserving schemes for magnetohydrodynamics. *Digital Comprehensive Summaries of Uppsala Dissertations from the Faculty of Science and Technology* 2414. 50 pp. Uppsala: Acta Universitatis Upsaliensis. ISBN 978-91-513-2165-3.

Magnetohydrodynamics (MHD) studies the behaviors of ionized gases, such as plasmas, in the presence of a magnetic field. MHD is used in many applications, such as geophysics, space physics, and nuclear fusion.

Despite intensive research in recent decades, many physical and numerical aspects of MHD are not well understood. The challenges inherent in solving MHD stem from the obstacles encountered in ordinary hydrodynamics, such as those described by the compressible Euler/Navier-Stokes equations, along with the intricacies arising from electromagnetism. A characteristic of compressible flows is their tendency to develop shocks/discontinuities over time. This often leads to unphysical traits in numerical approximations if the capturing scheme is not constructed properly. By physical laws, the magnetic field is solenoidal. However, in practice, numerical schemes seldom ensure this property precisely, which may lead to instability and convergence to wrong solutions. In numerical simulation of many applications, positive physical quantities such as density and pressure can easily become negative. On the whole, preserving the physical relevance of the numerical solutions poses a significant challenge in MHD.

This thesis presents several numerical schemes based on Galerkin approximations to solve MHD. The schemes rely on viscous regularization, a technique to remove mathematical singularities by adding a vanishing viscosity term to the MHD equations. At the continuous level, we propose several choices of viscous regularization and rigorously show that they are consistent with thermodynamics. Based on these choices, we construct numerical schemes of which robustness is confirmed through many challenging benchmarks. Finally, we propose a nonconventional algorithm that simultaneously preserves many desirable physical properties, including positivity of density and internal energy, conservation of total energy, minimum entropy principle, and zero magnetic divergence.

Keywords: MHD, magnetohydrodynamics, finite element method, artificial viscosity, viscous regularization, invariant domain

Tuan Anh Dao, Department of Information Technology, Division of Scientific Computing, Box 337, Uppsala University, SE-751 05 Uppsala, Sweden. Department of Information Technology, Numerical Analysis, Box 337, Uppsala University, SE-75105 Uppsala, Sweden.

ISSN 1651-6214
ISBN 978-91-513-2165-3
URN urn:nbn:se:uu:diva-532130 (http://urn.kb.se/resolve?urn=urn:nbn:se:uu:diva-532130)

Dedicated to Trúc

List of papers

This thesis is based on the following papers, which are referred to in the text by their Roman numerals.

I Tuan Anh Dao and Murtazo Nazarov. A high-order residual-based viscosity finite element method for the ideal MHD equations. *Journal of Scientific Computing*, 92(3):Paper No. 77, 24, 2022.

II Tuan Anh Dao and Murtazo Nazarov. Monolithic parabolic regularization of the MHD equations and entropy principles. *Computer Methods in Applied Mechanics and Engineering*, 398:Paper No. 115269, 25, 2022.

III Tuan Anh Dao and Murtazo Nazarov. A nodal based high order nonlinear stabilization for finite element approximation of magnetohydrodynamics. *Journal of Computational Physics*, Paper No. 113146, 2024.

IV Tuan Anh Dao, Lukas Lundgren, and Murtazo Nazarov. Viscous regularization of the MHD equations. Accepted for publication in *SIAM Journal on Applied Mathematics*.

V Tuan Anh Dao, Murtazo Nazarov, and Ignacio Tomas. A structure preserving numerical method for the ideal compressible MHD system. *Journal of Computational Physics*, 508:Paper No. 113009, 2024.

Related papers

The following papers, although not discussed in this thesis, were written during the author's time as a doctoral student.

VI Tuan Anh Dao, Ken Mattsson, and Murtazo Nazarov. Energy stable and accurate coupling of finite element methods and finite difference methods. *Journal of Computational Physics*, 449:Paper No. 110791, 25, 2022.

VII Ludvig Lindeberg, Tuan Dao, and Ken Mattsson. A high order accurate finite difference method for the Drinfel'd-Sokolov-Wilson equation. *Journal of Scientific Computing*, 88(1):Paper No. 18, 22, 2021.

Contents

Acknowledgments

First, I would like to express my heartfelt gratitude to my supervisor, Murtazo Nazarov, whose guidance and support have been invaluable throughout my PhD journey. His mentorship, encouragement, and unwavering dedication have profoundly impacted my personal and professional growth, making these past five years a deeply enriching and fulfilling experience.

I am grateful to have Ken Mattsson as my second supervisor, who introduced me to research in PDEs during my master's studies. Whenever I got dead stuck in a derivation, your positivity and knowledgeable insights always made me come back to my desk with excitement.

I would like to show my gratitude to Ignacio Tomas for the fruitful collaboration during Paper V, which were integral to the completeness of this thesis. My sincere appreciation also goes to Jean-Luc Guermond for his gracious hospitality and willingness to address my various questions during my visit to Texas A&M. I extend my thanks to Martin Kronbichler and Katharina Kormann for their warm welcome and valuable insights into high-performance implementations during my visit to RUB.

To Lukas Lundgren, I must be very lucky to have you as a colleague. I can't thank you enough for all the help I have received throughout these five years. Your exceptional work ethic and positive attitude have made our collaboration on Paper IV an absolute pleasure.

I am fortunate to be surrounded by great colleagues at TDB. Among those, I would like to mention Junjie Wen, Peter Munch, and Simon Sticko, and thank them for the Monday meetings with new ideas and constructive criticisms. I extend my appreciation to Gustav Eriksson, Vidar Stiernström, Martin Almquist, and Siang Wang for the discussions on SBP operators and for the 'wave meetings.' I also thank Zhenlu Sun for being a great office mate. I am truly grateful for the thoughtful advice from my extended supervisors Salman Toor, Andreas Hellander, and Anna Eckerdal. The administrative unit, particularly Anna-Lena Forsberg and Ulrika Jaresund, has provided great support, for which I am thankful. Special thanks go to Murtazo, Lukas, Peter, Maya Neytcheva, and Tùng for their thorough proofreading of this thesis.

I acknowledge the FEniCS [5] community for providing a convenient framework for finite element codes, which greatly facilitated the implementation of the schemes presented in Papers I-V. I am also thankful for the high-performance computing infrastructure provided by UPPMAX under project numbers SNIC 2021/22-233 and NAISS 2023/22-877. The financial

support from the Swedish Research Council (VR) under grant number 2021-04620 is gratefully acknowledged.

My life in Uppsala has been wonderful thanks to my Vietnamese friends: Tùng, Sơn, Đức Anh, anh Nam, Thuận, Lương, Điềm, Phong, Vi, Hùng Phan, Hùng Đoàn, Hoàng, Chương, Thanh Thanh, Hiếu, anh Phong, chị Lan - Magnus, anh Lâm - chị Thùy, anh Điệp - chị Dịu, anh Quý - chị Hà, anh Long - chị Hương, anh Long - chị Thái, anh Minh - chị Thủy, anh Tuấn - chị Oanh. Thank you for being such incredible companions and making my weekends so much fun!

Lastly, I would like to thank my mom and dad, without whom I wouldn't be the person I am today. Thank you for trusting my decisions and always being there for me. Ngân, you have been a wonderful sister who inspires me with your enthusiasm and learning aptitude; I am proud of you. Trúc, thank you for bringing color into my life, and thank you for making me a better person; you mean the world to me.

Sammanfattning på svenska

Fysikaliska processer kan studeras med hjälp av numeriska simuleringar. Området magnetohydrodynamik (MHD) grundades av den svenska fysikern Hannes Alfvén när han studerade norrsken, för vilket han belönades med ett Nobelpris 1970. Systemet med MHD-ekvationer är en fluidmodell som beskriver dynamiken hos joniserade gaser, såsom plasma, i närvaro av ett magnetfält.

Det har insetts att förståelse av MHD är särskilt användbart vid design av plasmainneslutning för fusionsreaktorer. För att generera positiv nettoenergi måste fusionsreaktorer innesluta plasma vid extremt höga temperaturer under tillräckligt lång tid. Det är allmänt accepterat att varje stabilt inneslutningssystem som varar mer än 100 μsek bör uppfylla MHD-ekvationerna. Därför är MHD:s roll att analysera och designa geometrier för magnetiska komponenter i inneslutningsanordningar. Att förverkliga fusionsreaktorer är ett av de mest efterfrågade och utmanande vetenskapliga projekten för mänskligheten idag. Tillämpningarna av MHD är också rikliga inom geofysik, rymdfysik och astrofysik. Till exempel används den för att studera solvindens interaktion med jordens magnetosfär, Mars, och månen; eller att studera plasmaflöden i solkoronan.

Bortsett från de vanliga svårigheterna inom beräkningsströmningsdynamik, såsom stabilitet, noggrannhet, nätgenerering och effektiv implementering, för att nämna några, är numeriska studier av MHD utmanande av flera andra skäl. Interaktionerna av MHD-vågorna är komplexa och den fysiska relevansen av dessa vågor är fortfarande en pågående debatt bland fysiker. Dessutom, om det numeriska magnetfältet förlorar sin solenoidala egenskap, kan simuleringarna bli instabila eller ge felaktiga lösningar, och trycket kan bli negativt. Målet med denna avhandling är att konstruera robusta numeriska metoder för MHD, som är *invariant-domän bevarande* (invariant-domain preserving, på engelska), det vill säga, de bibehåller fysikaliska egenskaper hos lösningarna, såsom positivitet hos densitet och tryck. Vi strävar också efter att säkerställa att magnetfältet är solenoidalt över tiden. De numeriska metoder som utvecklats i denna avhandling är beroende av *viskös regularisering*, en teknik som kan användas för att avlägsna matematiska singulariteter genom att lägga till ett försvinnande viskositetsvillkor till MHD-ekvationerna. Vi föreslår flera alternativ för viskös regularisering av MHD som är termodynamiskt kompatibla. Baserat på dessa tillämpas *artificiell viskositet* vid närheten av lösningens stötar/diskontinuiteter. Den artificiella viskositeten hjälper till att

stabilisera det numeriska schemat i närvaro av stötar/diskontinuiteter samtidigt som den bibehåller hög noggrannhet när lösningen är slät. Vi presenterar även en parameterfri metod, vilket underlättar för praktiker att använda metoden. De föreslagna numeriska metoderna fungerar mycket bra även på de mest utmanande referensproblemen.

På grund av tekniska skäl är det inte möjligt att konstruera invarianta domänbevarande scheman för MHD-ekvationssystemet i dess vanliga formulering. Från den kontinuerliga analysen insåg vi att magnetfältets evolution kan bortkopplas från MHD-systemets hydrodynamiska evolution. Därför delar vi evolutionen i två operatorer: den hydrodynamiska evolutionen och ett kopplat system av hastighet och magnetfält. På grund av detta kan vi använda de befintliga invarianta domänbevarande scheman för det hydrodynamiska evolutionen. Vi utformar sedan noggrant schemat som diskretiserar den andra operatorn och bevisar att hela schemat är invariant-domänbevarande. De nya formuleringarna tillåter speciell diskretisering av magnetfältet, vilket garanterar att det är solenoidiskt.

1. Background

1.1 Introduction

The field of magnetohydrodynamics (MHD) was pioneered by the Swedish physicist Hannes Alfvén [3] while studying aurora borealis, also known as the Northern lights, for which he was awarded a Nobel prize in 1970. The system of MHD equations is a single-fluid model to describe the dynamics of ionized gases, such as plasmas, in the presence of a magnetic field.

It was recognized that understanding MHD is particularly useful in designing plasma confinement for fusion reactors [32]. To generate positive net energy, fusion reactors must confine the plasma at extremely high temperatures for a sufficient amount of time. It is commonly agreed that every stable confinement system that lasts more than 100 μsec should satisfy the MHD equations. Therefore, the role of MHD is to analyze and design geometries of magnetic components in the confinement. The realization of fusion reactors is among the most sought-after and challenging scientific endeavors of humankind today [50, 70, 72].

The applications of MHD are also abundant in geophysics, space physics, and astrophysics [15]. For example, MHD is used to study the interaction of the solar wind with the Earth's magnetosphere [89] (which creates aurora), with Mars [57], and with the Moon [46]; or to study plasma flows in the solar corona [4, 63]. MHD also models various macroscopic plasma instabilities, such as Kelvin-Helmholtz instabilities [53, 66], Kink instabilities [82, 83], and Rayleigh-Taylor instabilities [76].

Apart from the common difficulties in computational fluid dynamics (CFD), such as stability, accuracy, mesh generation, and efficient implementation, to name a few, solving MHD is challenging for several additional reasons. The interactions of the MHD waves are complex, and the physical relevance of those waves is still an ongoing debate among physicists [84, 85, 96]. To make matters worse, the MHD solution in usual mathematical definitions is not unique even to the simplest one-dimensional shock problems [80]. Furthermore, if the numerical magnetic field loses its solenoidal property, the simulations may become unstable or may produce wrong solutions [14], and the numerical pressure may become negative [91].

Various numerical schemes for MHD have been developed using, for example, finite volume (FV) methods [28, 29, 90, 10], discontinuous Galerkin (DG) methods [34, 93, 94, 92], hybrid FV/discontinuous Galerkin spectral element methods (DGSEM) [13, 73], finite difference (FD) methods

[25, 65, 98], residual distribution (RD) methods [1, 2, 23, 24], and continuous Galerkin finite element (FE) methods [12, 52, 61]. Moreover, many solvers for specific applications have been developed for MHD: NIMROD [35], JOREK [45], RAMSES [33], Athena++ [77], LareXd [6]. These are by no means exhaustive lists.

This thesis aims to develop robust FE methods to solve MHD. Our goal is to build reliable and effective numerical schemes that preserve important physical properties.

The outline of this thesis is as follows. The rest of this chapter provides definitions and background knowledge for the remaining chapters. In Chapter 2, we describe the ideal MHD equations, together with useful definitions and properties. Viscous regularization and high-order viscosity finite element methods for MHD are discussed in Chapter 3. Chapter 4 describes a technique to simultaneously ensure the minimum entropy principle, the positivity of density and internal energy, and preserve the solenoidal nature of the magnetic field. Chapter 5 summarizes the scientific papers included in this thesis. The thesis is concluded in Chapter 6.

1.2 Conservation laws

Before discussing the more complex problem of the MHD equations, we examine a simpler model problem of scalar conservation laws.

Let Ω be an open bounded domain in $\mathbb{R}^d$, $(0, T]$ where $T > 0$ be a temporal domain, $u = u(\boldsymbol{x}, t) : \Omega \times (0, T] \to \mathbb{R}$ be the sought solution, and $\boldsymbol{f} : \mathbb{R} \to \mathbb{R}^d$ be a smooth function. We consider the following model problem described by a partial differential equation (PDE),

$$\begin{aligned} \partial_t u + \nabla \cdot \boldsymbol{f}(u) = 0, \quad (\boldsymbol{x}, t) \in \Omega \times (0, T], \\ u(\boldsymbol{x}, t) = u_0(\boldsymbol{x}), \quad \boldsymbol{x} \in \Omega, \end{aligned} \tag{1.1}$$

where proper boundary conditions are prescribed on the boundary $\partial\Omega$ of Ω and $u_0(\boldsymbol{x}) : \Omega \to \mathbb{R}$ is the initial solution. Based on the choice of the conserved variable u and the flux function $\boldsymbol{f}$, the equation (1.1) can describe the conservation of different physical quantities. For example, if u is a fluid density and $\boldsymbol{f}$ is the fluid momentum, then (1.1) describes the conservation of density/mass of the fluid. The equation (1.1) is called the *strong formulation*, and the solution u to (1.1) is referred to as the *strong solution*.

Over time, (1.1) even with a smooth initial solution may develop shocks/discontinuities, and a strong solution to (1.1) no longer exists. Therefore, we now introduce the notions of weak solution, viscosity solution, and entropy solution to (1.1). By multiplying (1.1) with a sufficiently smooth test function ϕ and integrating by parts, we obtain the *weak formulation*,

$$\int_0^T \int_\Omega (u \partial_t \phi + \boldsymbol{f}(u) \cdot \nabla \phi) \, \mathrm{d}\boldsymbol{x} \, \mathrm{d}t + \int_\Omega u_0(x) \phi(\boldsymbol{x}, 0) \, \mathrm{d}\boldsymbol{x} = 0. \tag{1.2}$$

A function u is called a *weak solution* to (1.1) if it satisfies (1.2) for all smooth compactly supported functions ϕ.

A convex function $S : \mathbb{R} \to \mathbb{R}$ and a mapping $\boldsymbol{q} : \mathbb{R} \to \mathbb{R}^d$ define an entropy pair if $\boldsymbol{q}_i'(u) = S'(u)\boldsymbol{f}_i'(u), i = 1, \ldots, d$. A solution u qualifies as an *entropy solution* to (1.1) if it is a weak solution to (1.1) and in addition, it fulfills the following *weak entropy condition*,

$$\int_0^T \int_\Omega (S(u)\partial_t\phi + \boldsymbol{q}(u)\cdot\nabla\phi)\,\mathrm{d}\boldsymbol{x}\,\mathrm{d}t + \int_\Omega S(u_0(x))\phi(\boldsymbol{x}, 0)\,\mathrm{d}\boldsymbol{x} \geq 0,$$

for all entropy pairs $(S, \boldsymbol{q})$ and for all smooth compactly supported nonnegative functions ϕ.

A function u^ε is called a *viscosity solution* to (1.1) if it is a solution of the following equation,

$$\partial_t u^\varepsilon + \nabla\cdot \boldsymbol{f}(u^\varepsilon) = \varepsilon\Delta u^\varepsilon, \tag{1.3}$$

where ε is a positive coefficient. The existence and uniqueness of a smooth solution u^ε to (1.3) is guaranteed [55, Chapter 11.6]. Furthermore, it is also known that u^ε converges to the entropy solution of (1.1) as $\varepsilon \to 0$ [55, Chapter 11.14]. Therefore, many numerical schemes construct ε as a vanishing coefficient as the mesh size goes to zero.

Next, we look at a nonlinear example of (1.2).

Example 1.1 (Burgers' equation)**.** Using a scalar notation f for the flux function $\boldsymbol{f}$ in 1D, we consider (1.1) with the following flux function,

$$f(u) = \frac{1}{2}u^2, \quad u_0 = \begin{cases} 1, & x < -1, \\ -x, & -1 \leq x < 0, \\ 0, & x \geq 0. \end{cases} \tag{1.4}$$

A usual way to investigate the solution of (1.4) is to look at the lines on the (x, t)–plane along which the solution remains unchanged, i.e., $\frac{\mathrm{d}}{\mathrm{d}t}u(x(t), t) = 0$. These are referred to as the *characteristic lines*. For (1.4), one can show that these lines are straight with slopes given by the initial data, $\frac{\mathrm{d}x(t)}{\mathrm{d}t} = u(x(t), t) = u_0(x)$. Now let us construct characteristic lines on the (x, t)–plane in Figure 1.1. Based on the characteristic lines, we obtain the solutions at different time points in Figure 1.2. Notice that before the critical time $t = 1$, the solution is time-reversible or, in other words, can be 'traced back' to the initial data following the characteristic lines.

At $t = 1$, the solution on $(-\infty, 0)$ and $(0, +\infty)$ is still well-defined by the values of u_0 on $(-\infty, -1)$ and $(0, +\infty)$. However, all the characteristic lines originated from $(-1, 0)$ intersect at one point. At this point, the single value of $u(x = 0, t = 1)$ is dictated by a range of values of u_0 on $[-1, 0]$. Thus, $\partial_x f(u(x = 0, t = 1))$ is indefinite, and the strong formulation (1.1) no longer makes sense when t reaches 1. In such a case, we have to look

at the weak formulation (1.2) and think in terms of weak solutions. Since there is a jump/discontinuity at $x = 0$, the solution at $t = 1$ is called a *shock wave*, or simply a *shock*. After $t = 1$, it can be shown that the unique entropy solution to (1.4) is the said shock propagating with a speed λ defined by the *Rankine-Hugoniot condition*,

$$f(u_L) - f(u_R) = \lambda(u_L - u_R),$$

where u_L and u_R are the left and right states of the discontinuity. Inserting $u_L = 1$ and $u_R = 0$ gives $\lambda = \frac{1}{2}$. This number determines the slope of the bold line in Figure 1.1. This example shows that even when f is smooth and the solution has sufficient regularity, this regularity can be lost in finite time.

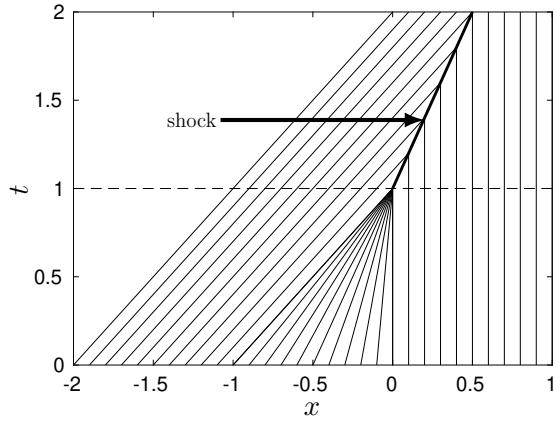

Figure 1.1. Characteristic lines on the (x, t)–plane in Example 1.1 (Burgers' equation). At $t = 1$, many characteristic lines cross at a singularity. From this time, strong solutions do not exist and the shock moves at the speed determined by the Rankine-Hugoniot condition.

To better understand the multi-dimensional problem (1.1), it is also common to study the following corresponding one-dimensional problem along a normalized direction vector $\boldsymbol{n}$, with a special setting of the initial condition,

$$\partial_t u + \partial_x(\boldsymbol{f}(u)\cdot\boldsymbol{n}) = 0, \quad u(\boldsymbol{x}, 0) = u_0 = \begin{cases} u_L, & x \le 0, \\ u_R, & x > 0. \end{cases} \tag{1.5}$$

The problem (1.5) is called a one-dimensional *Riemann problem*. The initial solution u_0 of (1.5) is entirely defined by two states: the left u_L and the right state u_R. In Example 1.1, the solution at $t = 1$ is an example of such an u_0 with $u_L = 1$ and $u_R = 0$. We denote the exact solution to (1.5) by $u(u_L, u_R, \boldsymbol{n})$. The *maximum wave speed*, denoted $\lambda_{\max} := \lambda_{\max}(u_L, u_R, \boldsymbol{n})$, refers to the largest speed of propagation of the solution to (1.5), i.e., the

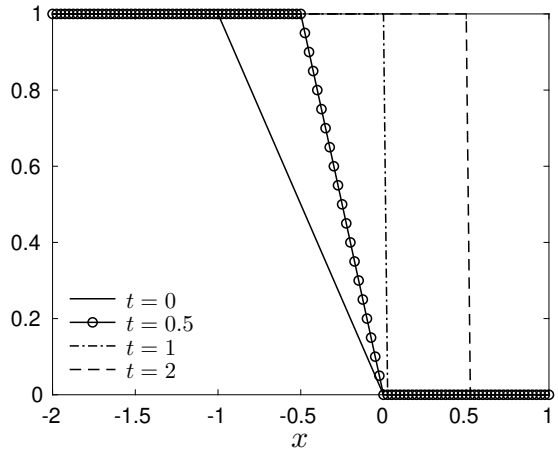

Figure 1.2. Weak solutions to the Burgers' equation in Example 1.1 at different time points. The shock is formed at $t = 1$.

smallest value of $\lambda_{\max} \in \mathbb{R}$ such that $u(u_L, u_R, \boldsymbol{n}) = u_L$ if $x/t \leq -\lambda_{\max}$ and $u(u_L, u_R, \boldsymbol{n}) = u_R$ if $x/t \geq \lambda_{\max}$. The quantity $\lambda_{\max}$ is important in the construction of the viscosity coefficient ε in numerical schemes. It also helps quantify the largest stable step size of an explicit time-stepping method.

2. The ideal MHD equations

In this chapter, we discuss the ideal MHD equations. First, we define a vector of conserved quantities $\mathbf{U} := (\rho, \boldsymbol{m}, E, \boldsymbol{B})^\top$, where $\rho, \boldsymbol{m}, E, \boldsymbol{B}$ denote *density, momentum, total energy*, and *magnetic field*, respectively. The *velocity* is defined as $\boldsymbol{u} := \frac{\boldsymbol{m}}{\rho}$. Let I denote the identity matrix of an appropriate size in each appearance. The ideal MHD equations can be written in a conservative form:

$$\begin{aligned} \partial_t \mathbf{U} + \nabla\cdot \mathbf{F}(\mathbf{U}) = 0, \quad (\boldsymbol{x}, t) \in \Omega \times (0, T], \\ \mathbf{U}(\boldsymbol{x}, t) = \mathbf{U}_0(\boldsymbol{x}), \quad \boldsymbol{x} \in \Omega, \end{aligned} \tag{2.1}$$

where the nonlinear advective flux is

$$\mathbf{F}(\mathbf{U}) := \begin{pmatrix} \boldsymbol{m} \\ \boldsymbol{m}\boldsymbol{u}^\top + \frac{1}{2}|\boldsymbol{B}|^2 - \boldsymbol{B}\boldsymbol{B}^\top + Ip \\ \boldsymbol{u}(E+p) + \left(\frac{1}{2}I|\boldsymbol{B}|^2 - \boldsymbol{B}\boldsymbol{B}^\top\right)\boldsymbol{u} \\ \boldsymbol{u}\boldsymbol{B}^\top - \boldsymbol{B}\boldsymbol{u}^\top \end{pmatrix}.$$

The *specific internal energy* e is defined as $e := \rho^{-1}E - \frac{1}{2}|\boldsymbol{u}|^2 + \frac{1}{2}\rho^{-1}|\boldsymbol{B}|^2$. The *total mechanical energy* is obtained by disregarding the magnetic contribution, $\mathcal{E} = E - \frac{1}{2}|\boldsymbol{B}|^2$. For simplicity, we consider ideal gases as the pressure p is determined by the following equation of state

$$p = (\gamma - 1)e, \tag{2.2}$$

and define the *specific entropy* s as

$$s = \ln \frac{p}{\rho^\gamma}, \tag{2.3}$$

where γ is the ideal gas constant. Let $S := \frac{\rho}{\gamma - 1}s$ be an *entropy*. Assuming that $\nabla\cdot \boldsymbol{B} = 0$, we obtain the following *entropy inequality*,

$$\partial_t S + \nabla\cdot(\boldsymbol{u}S) \geq 0. \tag{2.4}$$

Let $\mathcal{T}_h$ be a triangulation of Ω and $\mathcal{N}_h$ be the set of all nodal points in $\mathcal{T}_h$. For finite element discretization, let us define the finite element space $\boldsymbol{\mathcal{W}}_h := \mathcal{Q}_h \times \boldsymbol{\mathcal{V}}_h \times \mathcal{Q}_h \times \boldsymbol{\mathcal{H}}_h$, where $\mathcal{Q}_h$, $\boldsymbol{\mathcal{V}}_h$, and $\boldsymbol{\mathcal{H}}_h$ are the spaces from where we seek the solutions of ρ, $\boldsymbol{m}$, and $\boldsymbol{B}$, yet to be precisely defined. A finite element

approximation of (2.1) reads: find $\mathbf{U}_h(t) := (\rho_h(t), \boldsymbol{m}_h(t), E_h(t), \boldsymbol{B}_h(t))^\top \in C^1([0,T], \boldsymbol{\mathcal{W}}_h)$ such that

$$(\partial_t \mathbf{U}_h, \boldsymbol{\Phi}) + (\nabla \cdot \mathbf{F}(\mathbf{U}_h), \boldsymbol{\Phi}) = 0, \tag{2.5}$$

for all $\boldsymbol{\Phi} \in \boldsymbol{\mathcal{W}}_h$, where $(\cdot,\cdot)$ is the L^2–inner product over Ω.

The compressible Euler equations, which describe ordinary hydrodynamics, represent a special case of MHD when the magnetic field $\boldsymbol{B}$ is set to zero. In general, the Euler equations are well understood [55], but the addition of the magnetic field to MHD introduces considerable complexities. We discuss several properties of the MHD flux $\mathbf{F}$ in the next section.

2.1 Properties of the MHD flux

For a general flux function $\mathbf{F}(\mathbf{U})$, if the Jacobian matrix $\mathbf{F}'(\mathbf{U})$ is diagonalizable and has real eigenvalues, then the system (2.1) is called *hyperbolic*. If, in addition, the eigenvalues are distinct, then (2.1) is called *strictly hyperbolic*. Most of the definitions in Section 1.2 for conservation laws can be systematically generalized for hyperbolic systems. In the remainder of this thesis, we reuse the notions of shocks, weak formulation, weak solution, entropy condition, entropy solution, viscosity solution, Riemann problem, and maximum wave speed when discussing hyperbolic systems. We refer the interested readers to [30] for the precise corresponding definitions.

Let $\boldsymbol{n}$ be a normalized direction vector. We define the following quantities, the Alfvén speed c_a, the fast magnetoacoustic speed c_f, and the slow magnetoacoustic speed c_s,

$$\begin{aligned} c_a &:= \boldsymbol{B}\cdot\boldsymbol{n}/\rho^{\frac{1}{2}}, \\ c_{f,s}^2 &:= \frac{1}{2}\left(a^2 + \frac{\boldsymbol{B}^2}{\rho}\right) \pm \frac{1}{2}\left(\left(a^2 + \frac{\boldsymbol{B}^2}{\rho}\right)^2 - 4a^2 c_a^2\right), \end{aligned}$$

where $a := (\gamma p/\rho)^{\frac{1}{2}}$ is the speed of sound. The eigenvalues of the Jacobian matrix of (2.1) are

$$\lambda_{1,8} := \boldsymbol{u}\cdot\boldsymbol{n} \mp c_f, \lambda_{2,7} := \boldsymbol{u}\cdot\boldsymbol{n} \mp c_a, \lambda_{3,6} := \boldsymbol{u}\cdot\boldsymbol{n} \mp c_s, \lambda_{4,5} := \boldsymbol{u}\cdot\boldsymbol{n},$$

which are numbered in ascending order, $\lambda_1 \le \lambda_2 \le \cdots \le \lambda_8$. They correspond to eight elementary waves: two fast magnetoacoustic waves $\lambda_{1,8}$; two Alfvén waves $\lambda_{2,7}$; two slow magnetoacoustic waves $\lambda_{3,6}$; an entropy wave λ_4 and a divergence wave λ_5. The maximum wave speed is often taken as

$$\lambda_{\max} := \max_{i=1,\ldots,8} |\lambda_i| = \max(|\lambda_1|, |\lambda_8|). \tag{2.6}$$

Since at some spatial points it may happen that $c_f = c_a$ and/or $c_a = c_s$, the eigenvalues $\{\lambda_i\}_{i=1,\ldots,8}$ may coincide, yielding the non-strict hyperbolicity of the MHD equations [85]. The non-strict hyperbolicity of (2.1) and the non-convexity of $\mathbf{F}$ prevent uniqueness of the solution to be assured by the classical Lax theorem [54], see [80, 81, 84]. This is a notorious difficulty of MHD compared to other popular hyperbolic systems such as the compressible Euler equations or the shallow water equations [59]. As for the Euler counterpart, the unique solution can be obtained by limiting weak solutions to the entropy condition [18]. This is not the case for MHD. The MHD Riemann problem may simultaneously admit regular solutions in the sense of the Lax theorem [54], as well as non-regular solutions in special situations. An example of non-regular solutions to the Brio-Wu problem [17] is shown in Figure 2.1. Up to now, it is still inconclusive how to single out the physically relevant solution among the regular solution and the non-regular ones as this is an ongoing debate among mathematicians and physicists [81, 96]. Figure 2.1 also demonstrates the mystery of a specific non-regular solution to which almost all capable numerical schemes converge, including the schemes in Papers I-V. The reason why this happens is still unclear.

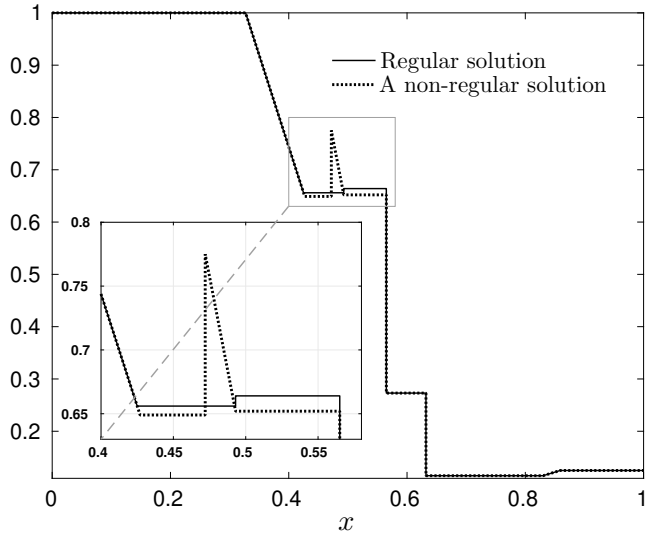

Figure 2.1. The regular Riemann solution of the Brio-Wu problem [17, 80], and one of the uncountably many non-regular solutions but to which almost all numerical codes converge

2.2 Divergence-free property of the magnetic field

A physical property of the magnetic field is that it is a solenoidal field, i.e.,

$$\nabla \cdot \boldsymbol{B} = 0. \tag{2.7}$$

This relation is not described by the ideal MHD equations (2.1). Nevertheless, applying a divergence operator to the fourth equation of (2.1), we obtain an additional evolutionary equation of the magnetic divergence $\nabla\cdot\boldsymbol{B}$,

$$\partial_t(\nabla\cdot\boldsymbol{B}) = 0, \tag{2.8}$$

which says that if the initial solution satisfies (2.7), then the solution should satisfy (2.7) at any time $t > 0$. In reality, a naive discretization of (2.1) does not automatically satisfy either (2.7) or (2.8). This turns out to be a serious issue. Even a small violation of (2.7) may lead to serious consequences [14, 91]. For example, the solver may break due to numerical instability or negativity of pressure, or wrong solutions may be obtained.

Because most MHD schemes do not guarantee exactly zero divergence, it is reasonable to reconsider the problem (2.1) with assuming $|\nabla\cdot\boldsymbol{B}| \neq 0$. In that case, to make the system compatible with thermodynamics, a non-conservative source term, often referred to as the "*Godunov/Powell term*" [36, 71], $\boldsymbol{\Psi} := -(\nabla\cdot\boldsymbol{B})\boldsymbol{S}(\boldsymbol{U})$, $\boldsymbol{S} = (0, \boldsymbol{B}, \boldsymbol{u}\cdot\boldsymbol{B}, \boldsymbol{u})^\top$ is added to the right-hand side of (2.1). Paper IV includes an analysis of the necessity of $\boldsymbol{\Psi}$ for entropy principles. The addition of $\boldsymbol{\Psi}$ is made at the cost of giving up conservativeness. The loss of conservativeness is, however, small and normally does not result in noticeable drawbacks if the divergence error $|\nabla\cdot\boldsymbol{B}|$ is kept small. To lower $|\nabla\cdot\boldsymbol{B}|$, various divergence cleaning techniques are proposed. The most straightforward approach is to bring the magnetic solution back to a divergence-free space after each time increment by a projection method [14]. Several other popular approaches are: hyperbolic cleaning [26], hyperbolic/parabolic [86] cleaning, constrained transport methods [20, 21, 34, 99], and locally divergence-free methods [56, 97]. Some of these techniques are compared in Paper I in the context of FE.

2.3 Invariant domain

Due to the existence of various definitions in the literature, we clarify what we mean by invariant sets and invariant domains, being the same as those in [30, 39].

Let $\boldsymbol{n}$ be a normalized direction vector. We consider the following one-dimensional Riemann problem,

$$\partial_t\mathbf{U} + \partial_x(\mathbf{F}(\mathbf{U})\cdot\boldsymbol{n}) = 0, \quad \mathbf{U}(\boldsymbol{x}, 0) = \begin{cases}\mathbf{U}_L, & x \leq 0,\\ \mathbf{U}_R, & x > 0.\end{cases} \tag{2.9}$$

We call $\mathcal{B}$ an *invariant set* for (2.1) if for any pair $(\mathbf{U}_L, \mathbf{U}_R) \in \mathcal{B}\times\mathcal{B}$, the vanishing viscosity solution to (2.9) remains in $\mathcal{B}$, for all $0 < t < \frac{1}{2\lambda_{\max}}$. As a

consequence, the average of the entropy solution to (2.9), $\frac{1}{2t\lambda_{\max}} \int_{-\lambda_{\max} t}^{\lambda_{\max} t} \mathbf{U}(\mathbf{U}_L, \mathbf{U}_R, \boldsymbol{n})\, \mathrm{d}\boldsymbol{x}$, also remains in $\mathcal{B}$ for all $0 < t < \frac{1}{2\lambda_{\max}}$.

Let us say we have a mapping S_h to increment an approximate solution $\mathbf{U}_h^n$ at time t_n to the next time level $\mathbf{U}_h^{n+1}$. A convex invariant set $\mathcal{A}$ is called an *invariant domain* for the mapping S_h if $\mathbf{U}_h^n$ in $\mathcal{A}$, then $\mathbf{U}_h^{n+1}$ is also in $\mathcal{A}$. For example, the space of positive densities,

$$\mathcal{A}_{\rho>0} := \{(\rho, \boldsymbol{m}, E, \boldsymbol{B})^\top \mid \rho > 0\}$$

is an invariant domain for Lax-Friedrichs-type and upwind schemes solving (2.5). In that case, the mapping S_h is called an invariant-domain preserving scheme in respect to the invariant domain $\mathcal{A}$.

To conclude this chapter, we summarize the main challenges in solving MHD for scientific and industrial applications, not in any particular order:

- high-order accuracy (at least second and above),
- numerical stability,
- computational efficiency,
- positivity of density and internal energy,
- discrete minimum entropy principle,
- discrete entropy stability in the spirit of (2.4),
- zero or virtually zero magnetic divergence,
- preservation of total energy.

With the current advances in solving MHD, the existing MHD schemes can address one or several of the properties above, but achieving them all together is extremely difficult.

3. High-order nonlinear viscosity methods

State-of-the-art FE schemes solving hyperbolic equations such as the compressible Euler or MHD often utilize linear stabilizations such as Galerkin Least Square (GLS) or Streamline Upwind Petrov-Galerkin (SUPG) methods, see [47]. These methods are, however, implicit by construction, technical to implement, and limited to second-order accuracy in space. This is perhaps the historical reason why DG, FV, and FD are often preferred over FE when solving hyperbolic equations. A way to break the second-order barrier to use an artificial viscosity method based on viscous regularization. This type of method dates back to the 50s in the work of Von Neumann and Richtmyer [87] which is known to be over dissipative. Recent years have witnessed advances in a class of artificial viscosity methods referred to as the entropy viscosity methods [22, 27, 37, 62], and the residual viscosity methods [60, 67, 68]. The main idea is to locally suppress the hyperbolic stiffness caused by strong shocks/discontinuities while leaving the high-order base scheme (nearly) unchanged in the smooth regions. These methods are robust, high-order accurate, computationally efficient, easy to implement, and can be made explicit in time, along with provable convergence, at least for scalar cases [67].

In this section, we describe several high-order artificial viscosity methods for MHD. First, two viscous regularizations are discussed: the monolithic parabolic regularization in Subsection 3.1.1, and the Guermond-Popov (GP) regularization in Subsection 3.1.2. In Sections 3.2, 3.3, 3.4 of this chapter, we discuss the constructions of high-order stable finite element methods using the mentioned viscous regularizations.

3.1 Viscous regularization

For viscous regularization, a viscosity term $\nabla\cdot \mathbf{F}_\varepsilon(\mathbf{U})$ should be added similarly to the term $\nabla\cdot(\varepsilon\nabla u)$ in the scalar equation (1.3), resulting in the following weak formulation

$$(\partial_t \mathbf{U}, \mathbf{\Phi}) + (\nabla\cdot \mathbf{F}(\mathbf{U}), \mathbf{\Phi}) + (\mathbf{F}_\varepsilon(\mathbf{U}), \nabla\mathbf{\Phi}) = 0, \tag{3.1}$$

where boundary terms are disregarded for simplicity. Unlike the scalar case, an incorrect construction of the viscosity term $\mathbf{F}_\varepsilon(\mathbf{U})$ may break energy balance and, consequently, violate entropy principles. Therefore, a mindful choice of $\mathbf{F}_\varepsilon(\mathbf{U})$ has to be made. For example, for the compressible Euler equations, thoughrough analyses for monolithic parabolic regularization have been carried out in [40, Section 5.1], [78, 79].

3.1.1 Monolithic parabolic regularization

Perhaps the simplest choice of $\mathbf{F}_\varepsilon(\mathbf{U})$ is the so-called *monolithic parabolic regularization* $\epsilon\nabla\mathbf{U}$, which can be written componentwise as

$$\mathbf{F}_\varepsilon^{\mathrm{m}}(\mathbf{U}) := \begin{pmatrix} \epsilon\nabla\rho \\ \epsilon\nabla\boldsymbol{m} \\ \epsilon\nabla E \\ \epsilon\nabla\boldsymbol{B} \end{pmatrix}, \ \epsilon > 0. \tag{3.2}$$

The continuous properties of $\mathbf{F}_\varepsilon^{\mathrm{m}}$ are analyzed in Paper II. While $\mathbf{F}_\varepsilon^{\mathrm{m}}$ may appear arbitrary at first glance, it proves to be an effective choice for viscous regularization. In contrast to the commonly used physically-motivated model "*resistive MHD*", under reasonable assumptions, the monolithic flux guarantees positivity of density and internal energy, ensures the minimum entropy principle, and is compatible with many entropy inequalities. See the definition of the resistive MHD model in Paper II. From the numerical point of view, $\mathbf{F}_\varepsilon^{\mathrm{m}}$ is a continuous analog to the well-known Lax-Friedrichs or the upwind scheme. However, some disadvantages are that it is unclear how to incorporate physical viscosities into $\mathbf{F}_\varepsilon^{\mathrm{m}}$; and angular momentum $\int_\Omega \boldsymbol{m} \times \boldsymbol{x} \, \mathrm{d}\boldsymbol{x}$ is not conserved, despite being an important physical property.

3.1.2 Guermond-Popov viscous regularization

To overcome the aforementioned drawbacks of the monolithic flux, we proposed a physically-motivated viscous regularization of MHD in Paper IV. The new choice of regularization possesses all of the beneficial properties of $\mathbf{F}_\varepsilon^{\mathrm{m}}$. It is a combination of the GP flux [40] for fluid flows, and the resistive MHD model for the magnetic components,

$$\mathbf{F}_\varepsilon^{\mathrm{GP}}(\mathbf{U}) := \begin{pmatrix} \kappa\nabla\rho \\ \mu\rho\nabla^s\boldsymbol{u} + (\kappa\nabla\rho)\otimes\boldsymbol{u} \\ \kappa\nabla(\rho e) + \frac{|\boldsymbol{u}|^2}{2}\kappa\nabla\rho + \mu\rho(\nabla^s\boldsymbol{u})\boldsymbol{u} + \eta\big(\nabla\boldsymbol{B} - \nabla\boldsymbol{B}^\top\big)\boldsymbol{B} \\ \eta\big(\nabla\boldsymbol{B} - \nabla\boldsymbol{B}^\top\big) \end{pmatrix}, \tag{3.3}$$

where $\nabla^s = \frac{1}{2}(\nabla + \nabla^\top)$, and κ, μ, η are different positive viscosity coefficients. From a physical standpoint, inherited from the GP flux, $\mathbf{F}_\varepsilon^{\mathrm{GP}}$ can be related to the recent nonconventional physical model of fluid flows proposed by Howard Brenner [16, 31]. Brenner's model has received both interest and criticism from the related fields of physics. The strongest criticism is perhaps the loss of conservation of angular momentum [69]. Therefore, we proposed an angular momentum conserving variation of $\mathbf{F}_\varepsilon^{\mathrm{GP}}$,

defined as

$$\mathbf{F}_{\varepsilon}^{\mathrm{GP}^s}(\mathbf{U}) := \begin{pmatrix} \kappa\nabla\rho \\ \mu\rho\nabla^s\boldsymbol{u} + \frac{1}{2}((\kappa\nabla\rho)\otimes\boldsymbol{u} + \boldsymbol{u}\otimes(\kappa\nabla\rho)) \\ \kappa\nabla(\rho e) + \frac{|\boldsymbol{u}|^2}{2}\kappa\nabla\rho + \mu\rho(\nabla^s\boldsymbol{u})\boldsymbol{u} + \eta\big(\nabla\boldsymbol{B} - \nabla\boldsymbol{B}^\top\big)\boldsymbol{B} \\ \eta\big(\nabla\boldsymbol{B} - \nabla\boldsymbol{B}^\top\big) \end{pmatrix}. \tag{3.4}$$

The viscous regularization (3.4) indeed conserves angular momentum. When $\mathbf{F}^{\mathrm{GP}^s}$ is used, a small energy compensation needs to be added to the right-hand side to make the entropy inequalities hold,

$$\mathbf{F}^{E}(\mathbf{U}) := \begin{pmatrix} 0 \\ 0 \\ \frac{1}{2}\left(\nabla\cdot\left(\boldsymbol{u}\otimes(\kappa\nabla\rho) - (\kappa\nabla\rho)\otimes\boldsymbol{u}\right)\right)\cdot\boldsymbol{u} \\ 0 \end{pmatrix}. \tag{3.5}$$

Therefore, $\mathbf{F}_{\varepsilon}^{\mathrm{GP}^s}$ is compliant with all the positivity and entropy principles, angular-momentum conserving, but only 'nearly' energy conservative. In one dimension, $\mathbf{F}^{E}$ is identically zero and $\mathbf{F}_{\varepsilon}^{\mathrm{GP}^s} \equiv \mathbf{F}_{\varepsilon}^{\mathrm{GP}}$.

An example demonstrating the advantages of the two proposed viscous regularizations over the conventional resistive MHD model is shown in Figure 3.1. The test problem contains a contact line, a challenging MHD Riemann setting described in Paper II. A first-order Lax-Friedrichs-type density solution to this problem should respect the bounds of the initial solution. This expectation is not delivered by the resistive MHD model. In contrast, the monolithic and the GP regularizations yield the expected behavior.

3.2 Entropy viscosity method

In this section we describe a typical construction of an entropy viscosity (EV) method. The equality in the entropy inequality (2.4) holds if the solution is smooth. The inequality sign applies at discontinuities. Therefore, the entropy residual can be used as a shock indicator which we use to construct artificial viscosity. This is the main idea of the EV method. The EV method is employed in Paper II. We start by constructing a first-order viscosity as a safety upper bound of the artificial viscosity at each nodal point,

$$\varepsilon_i^L := C_{\max} h_i \lambda_{\max,i}, \tag{3.6}$$

for $i \in \mathcal{N}_h$, where $C_{\max}$ is a real number usually chosen to be $\frac{1}{2}$; h_i is a mesh-size indicator at node i; and $\lambda_{\max,i}$ is calculated by (2.6) at node i. Assuming sufficiently small time step in the order of $\mathcal{O}(h)$ and that $\lambda_{\max,i}$ is a sufficiently large approximation of the maximum wave speed at node i, ε^L

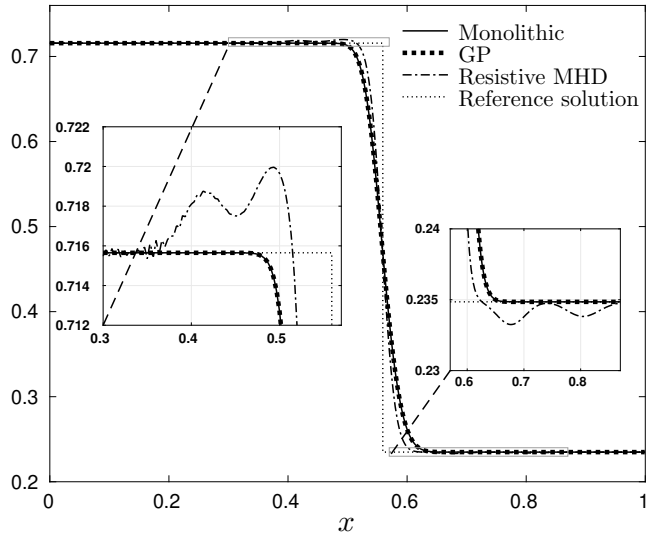

Figure 3.1. First-order viscosity finite element solutions for the contact problem in Paper II using different viscous regularizations: monolithic, GP, and resistive MHD. The solutions are discretized with 300 mesh points. The resistive MHD flux produces upper and lower bound violations while the other two do not. The monolithic flux and the GP flux solutions are almost identical in this test.

ensures invariant-domain preservation but delivers at best first-order accuracy. Let s_h be the specific entropy solution calculated by (2.3) and $s_{h,i}$ is the value of s_h at node i. To achieve high-order accuracy, we construct the high-order viscosity based on the entropy residual (2.4), determined at each nodal point $i \in \mathcal{N}_h$ as

$$\varepsilon_i^H := C_E h_i^2 \frac{|R_i(\boldsymbol{u}_h)|}{\|s_{h,i} - \bar{s}_h\|_{\infty,\Omega}},$$

where the parameter C_E is usually chosen to be 1, R_i is the nodal value of $R(\boldsymbol{u}_h)$ being an exact or approximate calculation of the left-hand side of (2.4), and $\bar{s}_h$ is the global average of s_h. The denominator is to normalize the units of ε^H. Finally, the artificial viscosity is constructed as

$$\varepsilon_i = \min(\varepsilon_i^L, \varepsilon_i^H),$$

for every nodal point $i \in \mathcal{N}_h$. The viscosity coefficients ϵ in (3.2), and κ, μ, η in (3.3) can be set the same or proportionally to ε.

3.3 Residual viscosity method

The residual viscosity (RV) method belongs to the same family as the EV method, where the residual of the PDE is used in place of the entropy residual. Convergence to the unique entropy solution of the RV method for

scalar conservation laws with implicit Euler time-stepping and FE discretization in space is shown by [67]. One advantage of using the RV method over the EV method is that for some equations with complicated or tabulated equations of states, for example [22], constructing the entropy residual can be inconvenient, but the residual of the PDE is always available from the scheme construction. The RV method is demonstrated in Papers I, III, and IV. Below, we briefly describe the RV method for MHD.

The first-order viscosity ϵ_i^L is constructed similarly to (3.6). Again, we use the subscript i to refer to the corresponding nodal values. The high-order viscosity is computed by taking the maximum of all residuals of the conservation equations,

$$\varepsilon_i^H := C_E h_i^2 \max \left\{ \frac{|R_{\rho,i}(\mathbf{U}_h)|}{n_i(\rho_h)}, \frac{|R_{\boldsymbol{m},i}(\mathbf{U}_h)|}{n_i(\boldsymbol{m}_h)}, \frac{|R_{E,i}(\mathbf{U}_h)|}{n_i(E_h)}, \frac{|R_{\boldsymbol{B},i}(\mathbf{U}_h)|}{n_i(\boldsymbol{B}_h)} \right\},$$

where the parameter C_E is usually chosen to be 1; $R_\rho(\mathbf{U}_h), R_{\boldsymbol{m}}(\mathbf{U}_h), R_E(\mathbf{U}_h)$, and $R_{\boldsymbol{B}}(\mathbf{U}_h)$ are the residuals of the conservation equations corresponding to each conserved variable in the subscripts; and $n(\rho_h), n(\boldsymbol{m}_h), n(E_h)$, and $n(\boldsymbol{B}_h)$ normalize the units of the corresponding residuals. The residuals $R_\rho, R_{\boldsymbol{m}}, R_E, R_{\boldsymbol{B}}$ can be the standard finite element projection such as in Paper I, or a projection with elliptic smoothing such as in Paper III. A conventional choice of the normalization function n is similar to the described EV formulation, for instance $n(\rho) := \|\rho_h - \bar{\rho}_h\|_{\infty,\Omega}$, where $\bar{\rho}_h$ is the global average of ρ_h. Two improved alternatives of n are proposed in Paper I and III, although not presented here for readability. Then again at every nodal point, the artificial viscosity is set as

$$\varepsilon_i = \min(\varepsilon_i^L, \varepsilon_i^H).$$

The viscosity coefficients ϵ in (3.2), and κ, μ, η in (3.3) can be set the same or proportionally to ε.

3.4 Parameter-free viscosity construction

In the FE context, the definition of the mesh-size indicator h in the construction of the artificial viscosity coefficient ε is uncertain, especially when the mesh is unstructured. Depending on the particular definition of h and the benchmark problem, the coefficient $C_{\max}$ may require adjustment to enhance outcome [37]. Therefore, our aim in Paper III is to create a high-order viscosity method that does not require any tunable parameters. A way to achieve this is using the graph viscosity described in Section 4.2. Using graph viscosity, a matrix of viscosity coefficients $\varepsilon_{ij},\ i,j \in \mathcal{N}_h$ needs to be recomputed before each time increment, and becomes dense for high-order elements. In contrast, the work of Paper III describes a no-tuning approach that only requires viscosity

calculation and storage at each nodal point $i \in \mathcal{N}_h$. The key to this approach is a novel parameter-free first-order invariant-domain preserving scheme based on a sub-mesh of which mesh points coincide with the nodal points of the finite element solution. An example of such a sub-mesh for a mesh containing one $\mathbb{P}_3$ element is demonstrated in Figure 3.2.

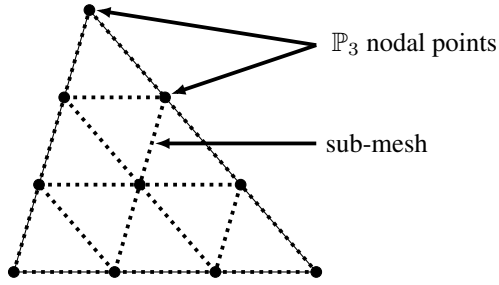

Figure 3.2. Example of a sub-mesh construction in Paper III on a single $\mathbb{P}_3$ element. The straight lines are the edges of the $\mathbb{P}_3$ element. The big black dots are the nodal points of this $\mathbb{P}_3$ element. The dotted line is the sub-mesh which is used to construct the parameter-free artificial viscosity.

Let us consider $\mathcal{Q}_h$ a space of piecewise Lagrange polynomials. Set $\mathcal{V}_h \equiv \mathcal{H}_h := [\mathcal{Q}_h]^d$. Let $m_i^{\mathbb{P}_1,\text{sub}}$ be the lumped mass $m_i^{\mathbb{P}_1,\text{sub}} := \int_\Omega \varphi_i^{\mathbb{P}_1,\text{sub}} \, \mathrm{d}\boldsymbol{x}$ of the piecewise linear Lagrange basis functions $\varphi_i^{\mathbb{P}_1,\text{sub}}$ defined on the corresponding sub-mesh of $\mathcal{Q}_h$. Denote $\mathcal{I}^{\text{sub}}(i)$ the set of the connected vertices to a node i on the sub-mesh, and S_i the set of all elements sharing node i. The first-order viscosity is formulated as

$$\varepsilon_i^L = C_i m_i^{\mathbb{P}_1,\text{sub}} \lambda_{\max,i}(\mathbf{U}_h) \varphi_i^{\mathbb{P}_1,\text{sub}},$$

where $\lambda_{\max,i}$ is the nodal maximum wave speed approximated by the eigenvalues of the MHD system similarly to (2.6),

$$\lambda_{\max,i} := \max_{i \neq j \in \mathcal{I}^{\text{sub}}(i)} \max\{\lambda_1(\mathbf{U}_h), \lambda_8(\mathbf{U}_h)\};$$

and C_i is a well-defined nodal coefficient computed once at the start of the simulation,

$$C_i := \frac{d+1}{2} \frac{1}{N_{el}(S_i)} \max_{K \in S_i} |K|^{-1},$$

where $N_{el}(S_i)$ is the number of elements in S_i, and $|K|$ is the area of the element K. For scalar equations, we rigorously prove in Paper III that ε_i^L is sufficient to preserve positivity under a regular CFL condition.

A high-order nonlinear viscosity method such as EV or RV is then incorporated to gain accuracy. The final artificial viscosity is given at each nodal point by

$$\varepsilon_i := C_i \min \left\{ \lambda_{\max,i}(\mathbf{U}_h) \varphi_i^{\mathbb{P}_1,\text{sub}}, \frac{|R_i(\mathbf{U}_h)|}{n_i(\mathbf{U}_h)} \right\} m_i^{\mathbb{P}_1,\text{sub}},$$

where $\frac{|R_i(\mathbf{U}_h)|}{n_i(\mathbf{U}_h)}, i \in \mathcal{N}_h$ are the nodal values of the normalized entropy residual or the PDE residual.

4. Invariant-domain preservation

Due to discretization errors, numerical approximations of positive physical quantities such as density and pressure may become negative. In that case, the physics breaks down and the numerical solutions are deemed useless. There are many situations when positivity preservation becomes crucial: near vacuum states, low-density fluids, high Mach flows, strong discontinuities, physical instabilities, and low plasma-beta flows, i.e., the ratio of pressure to magnetic strength is very small. Such situations are not rare in real applications [46, 63, 75]. Unfortunately, the majority of MHD schemes do not guarantee this property, including the ones presented in Papers I and III.

It is no surprise that many attempts have been made to achieve the positivity of density, pressure, and internal energy. Pioneering attempts include [9, 11, 48, 88]. Most of them involve carefully designing 1D Riemann solvers and applying reconstruction techniques. This is followed by the recent advances of positivity-preserving schemes using FV [28], DG [93, 94, 95, 99], central DG [19, 58, 92], FD [20, 21], FE [52]. Many new insights into positivity properties are revealed, for example, the strong connection of positivity with the divergence condition [91], or the necessity of correctly discretizing a non-conservative divergence source term.

Despite experimental evidence of robustness in Papers I-IV, several obstacles in constructing a true positivity-preserving scheme remain in our case. One fundamental issue is the efficient calculation of the maximum wave speed $\lambda_{\max}$ or a close-enough upper bound of it. The value of $\lambda_{\max}$ appears in several basic components of a positivity-preserving scheme such as the low-order Lax-Friedrichs-type scheme, and the time step size. As described in (2.6), $\lambda_{\max}$ is often approximated by the maximum absolute value of the eigenvalues of the MHD system. This commonly used approximation is surprisingly unreliable. An example can be taken from the system of the compressible Euler equations, which is a special case of MHD when the fluid is non-conducting, i.e., $\boldsymbol{B} \equiv 0$. In this case, [41] shows that the exact $\lambda_{\max}$ may exceed multiple times of the approximation (2.6). The unavailability of an efficient algorithm for $\lambda_{\max}$ poses an impediment to constructing a positivity-preserving scheme for MHD.

Our technique in Paper V to address the positivity preservation of MHD is fundamentally different from the aforementioned existing works. First, the interaction of the magnetic field $\boldsymbol{B}$ is separated from the hydrodynamic evolution. The scheme requires two separate discretizations: a source system discretization to account for the interaction of $\boldsymbol{m}$ and $\boldsymbol{B}$, and a compressible

Euler discretization to increment $\rho, \boldsymbol{m}, E$ in time. In this way, we avoid the two biggest problems: neither a Riemann solver nor the maximum wave speed $\lambda_{\max}$ of MHD is used. Positivity preservation is contained in the more general concept of an invariant domain in which the solution is guaranteed to stay by a limiting procedure. The limiting procedure is called *convex limiting* [39]. As opposed to the flux-corrected transport method [51] which addresses box constraints, convex limiting can be applied on general convex invariant sets. For example, it can be used to enforce the minimum entropy principle. The solution procedure described here makes use of good existing compressible Euler solvers and can be adapted to many existing numerical methods, see [43] and Paper V. Furthermore, the scheme preserves the solenoidal property of $\boldsymbol{B}$ in the weak meaning of (2.8): the weak divergence of the magnetic field remains zero if the initial weak divergence is zero. The remainder of this section explains conceptually the proposed scheme in Paper V.

To turn readers' attention to the scenario considered in Paper V, we define the following invariant domain of (2.1),

$$\mathcal{A} := \{(\rho, \boldsymbol{m}, E, \boldsymbol{B})^\top \mid \rho > 0, e > 0, s \geq \min(s_0)\}.$$

It can be shown that $\mathcal{A}$ is a convex set [74]. In the case of ideal gases, $\rho > 0$ and $e > 0$ yield $p > 0$ due to the relation $p = (\gamma - 1)\rho e$.

4.1 Source system formulation and Strang-splitting

A non-conservative formulation of (2.1) without the divergence-free assumption $\nabla \cdot \boldsymbol{B} = 0$ is

$$\begin{aligned} \partial_t \rho + \nabla \cdot \boldsymbol{m} &= 0, \\ \partial_t \boldsymbol{m} + \nabla \cdot (\boldsymbol{m}\boldsymbol{u}^\top + \mathcal{I}p) &= -\boldsymbol{B} \times (\nabla \times \boldsymbol{B}), \\ \partial_t \mathcal{E} + \nabla \cdot (\boldsymbol{u}(\mathcal{E} + p)) &= -(\boldsymbol{B} \times (\nabla \times \boldsymbol{B})) \cdot \boldsymbol{u}, \\ \partial_t \boldsymbol{B} &= \nabla \times (\boldsymbol{u} \times \boldsymbol{B}), \end{aligned} \tag{4.1}$$

where the terms related to $\boldsymbol{B}$ are moved to the right-hand side.

The evolution of (4.1) can be split into two operators using the Strang-splitting. The first operator is

$$\text{Operator \#1:} \qquad \begin{aligned} \partial_t \rho + \nabla \cdot \boldsymbol{m} &= 0, \\ \partial_t \boldsymbol{m} + \nabla \cdot (\boldsymbol{m}\boldsymbol{u}^\top + \mathcal{I}p) &= \boldsymbol{0}, \\ \partial_t \mathcal{E} + \nabla \cdot (\boldsymbol{u}(\mathcal{E} + p)) &= 0, \\ \partial_t \boldsymbol{B} &= \boldsymbol{0}. \end{aligned} \tag{4.2}$$

Because the last equation of (4.2) is decoupled and has a trivial solution, solving (4.2) is equivalent to solving the system of the compressible Euler

equations. The second stage concerns the remaining terms on the right hand side of (4.1),

$$\text{Operator \#2:} \qquad \begin{aligned} \partial_t \rho &= 0, \\ \partial_t \boldsymbol{m} &= -\boldsymbol{B} \times \nabla \times \boldsymbol{B}, \\ \partial_t \mathcal{E} &= -(\boldsymbol{B} \times \nabla \times \boldsymbol{B}) \cdot \boldsymbol{u}, \\ \partial_t \boldsymbol{B} &= \nabla \times (\boldsymbol{u} \times \boldsymbol{B}). \end{aligned} \tag{4.3}$$

In (4.3), only the second and the fourth equations are coupled, the momentum and the magnetic field can be solved separately,

$$\begin{aligned} \partial_t \boldsymbol{m} &= -\boldsymbol{B} \times \nabla \times \boldsymbol{B}, \\ \partial_t \boldsymbol{B} &= \nabla \times (\boldsymbol{u} \times \boldsymbol{B}). \end{aligned} \tag{4.4}$$

We call the second equation in (4.4) the induction equation, and (4.4) the source system.

Figure 4.1 describes a usual Strang-splitting scheme. It involves three solution updates to increment the solution from time step t^n to t^{n+1}: an Euler update advancing Operator #1 described in (4.2) using time-step τ determined by the CFL condition of the Euler system; a source update advancing Operator #2 described in (4.3) using the double time-step 2τ together with a procedure to update the total energy; then finally another Euler update advancing Operator #1 using time-step τ.

An invariant-domain preserving scheme for the first and the third updates is described later in Section 4.2. The first Euler update increments the solution $\{\rho_h^n, \boldsymbol{m}_h^n, \mathcal{E}_h^n\}$ at t^n to the intermediate state $\{\rho_h^1, \boldsymbol{m}_h^1, \mathcal{E}_h^1\}$, setting $\boldsymbol{B}_h^1 \equiv \boldsymbol{B}_h^n$. Now, we discuss the second update to obtain $\{\rho_h^2, \boldsymbol{m}_h^2, \mathcal{E}_h^2, \boldsymbol{B}_h^2\}$ from $\{\rho_h^1, \boldsymbol{m}_h^1, \mathcal{E}_h^1, \boldsymbol{B}_h^1\}$. By (4.3), we set $\rho_h^2 \equiv \rho_h^1$. Let $(\boldsymbol{z}_h, \boldsymbol{\mathcal{X}}_h) \in \boldsymbol{\mathcal{V}}_h \times \boldsymbol{\mathcal{H}}_h$ be sufficiently smooth test functions. Using the Crank-Nicolson method, a weak formulation of (4.4) reads

$$\begin{aligned} \int_\Omega (\rho_h^2 \boldsymbol{u}_h^2 - \rho_h^1 \boldsymbol{u}_h^1) \cdot \boldsymbol{z}_h \,\mathrm{d}\boldsymbol{x} &= -2\tau \int_\Omega \left(\boldsymbol{B}_h^{\frac{1}{2}} \times (\nabla \times \boldsymbol{B}_h^{\frac{1}{2}}) \right) \cdot \boldsymbol{z}_h \,\mathrm{d}\boldsymbol{x}, \\ \int_\Omega (\boldsymbol{B}_h^2 - \boldsymbol{B}_h^1) \cdot \boldsymbol{\mathcal{X}}_h \,\mathrm{d}\boldsymbol{x} &= 2\tau \int_\Omega (\boldsymbol{B}_h^{\frac{1}{2}} \times (\nabla \times \boldsymbol{\mathcal{X}}_h)) \cdot \boldsymbol{u}_h^{\frac{1}{2}} \,\mathrm{d}\boldsymbol{x}, \end{aligned}$$

where $\boldsymbol{B}_h^{\frac{1}{2}} := \frac{1}{2}(\boldsymbol{B}_h^1 + \boldsymbol{B}_h^2)$, $\boldsymbol{u}_h^{\frac{1}{2}} := \frac{1}{2}(\boldsymbol{u}_h^1 + \boldsymbol{u}_h^2)$. This system can be solved by Newton's iteration. The total energy $\mathcal{E}_i^2$ satisfying the third equation of (4.3) can be obtained by a simple calculation at each nodal point i,

$$\mathcal{E}_i^2 = \mathcal{E}_i^1 - \frac{1}{2}\rho_i^1 (\boldsymbol{u}_i^1 \cdot \boldsymbol{u}_i^1) + \frac{1}{2}\rho_i^2 (\boldsymbol{u}_i^2 \cdot \boldsymbol{u}_i^2).$$

The last Euler update increments the solution from the second intermediate state $\{\rho_h^2, \boldsymbol{m}_h^2, \mathcal{E}_h^2\}$ to $\{\rho_h^{n+1}, \boldsymbol{m}_h^{n+1}, \mathcal{E}_h^{n+1}\}$. Since the magnetic field solution does not change in the third update, we simply set $\boldsymbol{B}_h^{n+1} \equiv \boldsymbol{B}_h^2$.

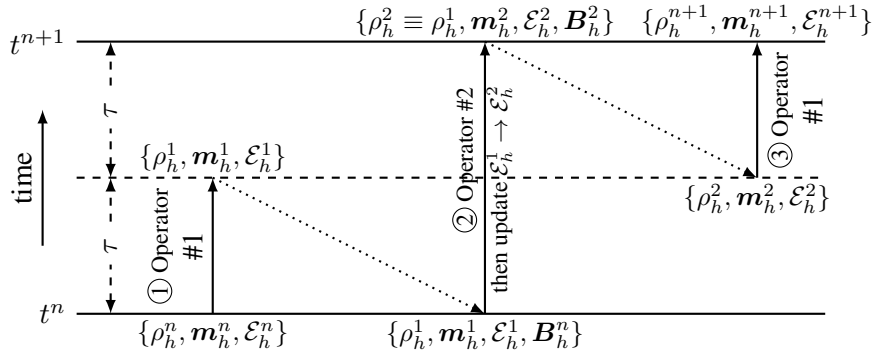

Figure 4.1. Diagram of the time-stepping scheme using the Strang-splitting to increment the solution from time t^n to $t^{n+1} = t^n + 2\tau$

4.2 Invariant-domain preservation by convex limiting

In this section we describe the technique used in Paper V to achieve second-order accuracy, the positivity of density and internal energy, and the discrete minimum entropy principle for the Euler solution. It requires three ingredients: (i) a low-order Lax-Friedrichs-type invariant-domain preserving scheme, (ii) a high-order entropy-consistent scheme, and (iii) a limiting procedure to enforce the invariant-domain constraints on the high-order solution. By "entropy consistency", we mean any scheme in which the solution evidently converges toward the entropy solution.

Now, we consider the system of the compressible Euler equations. We abuse the same notations for the solution vector $\mathbf{U} := (\rho, \boldsymbol{m}, \mathcal{E})^\top$, where the conserved variables $\rho, \boldsymbol{m}, \mathcal{E}$ have the same meaning as those in Chapter 2. The system of the compressible Euler equations reads

$$\partial_t \mathbf{U} + \nabla \cdot \mathbb{F}(\mathbf{U}) = 0, \quad \mathbb{F}(\mathbf{U}) := \begin{pmatrix} \boldsymbol{m} \\ \boldsymbol{m}\boldsymbol{u}^\top + \mathcal{I}p \\ \boldsymbol{u}(\mathcal{E} + p) \end{pmatrix},$$

where $\boldsymbol{u} := \frac{\boldsymbol{m}}{\rho}$ is again the velocity and the pressure p is defined by the equation of state (2.2). Recall that I is the identity matrix. At each point in time, we seek the finite element solutions in $\boldsymbol{\mathcal{W}}_h := \mathcal{Q}_h \times \boldsymbol{\mathcal{V}}_h \times \mathcal{Q}_h$.

To obtain a convenient formulation for the positivity-preserving scheme, instead of the regular Laplacian operator for artificial dissipation, we use the so-called *graph viscosity*, see [42, 39]. Let $\mathcal{Q}_h$ be the space of piecewise linear functions spanned by the linear Lagrange basis functions $\{\varphi_i\}_{i \in \mathcal{N}_h}$ and set $\mathcal{V}_h := [\mathcal{Q}_h]^d$. Let us introduce two new quantities,

$$\boldsymbol{c}_{ij} := \int_\Omega (\nabla \varphi_j) \varphi_i \, \mathrm{d}\boldsymbol{x}, \quad \boldsymbol{n}_{ij} := \frac{\boldsymbol{c}_{ij}}{\|\boldsymbol{c}_{ij}\|}, \quad i, j \in \mathcal{N}_h,$$

where $\|\cdot\|$ denotes the discrete l^2-norm. The integral $\int_\Omega \nabla\cdot\mathbb{F}(\mathbf{U}_h^n)\varphi_i\,\mathrm{d}\boldsymbol{x}$ can then be approximated by $\sum_{j\in\mathcal{I}(i)}\mathbb{F}(\mathbf{U}_j^n)\boldsymbol{c}_{ij}$. The low-order scheme with graph viscosity is formulated as

$$m_i\frac{\mathbf{U}_i^{L,n+1}-\mathbf{U}_i^n}{\tau}+\sum_{j\in\mathcal{I}(i)}\left(\mathbb{F}(\mathbf{U}_j^n)\boldsymbol{c}_{ij}-\boldsymbol{d}_{ij}^L(\mathbf{U}_j^n-\mathbf{U}_i^n)\right)=\mathbf{0}, \tag{4.5}$$

where $m_i:=\int_\Omega\varphi_i\,\mathrm{d}\boldsymbol{x}$ is the lumped mass, and $\boldsymbol{d}_{ij}^L$ are the first-order graph viscosity coefficients,

$$\boldsymbol{d}_{ji}^L=\boldsymbol{d}_{ij}^L:=\max(\lambda_{\max}(\mathbf{U}_i^n,\mathbf{U}_j^n,\boldsymbol{n}_{ij})\|\boldsymbol{c}_{ij}\|,\lambda_{\max}(\mathbf{U}_j^n,\mathbf{U}_i^n,\boldsymbol{n}_{ji})\|\boldsymbol{c}_{ji}\|),$$

for $i\neq j$, and

$$\boldsymbol{d}_{ii}^L:=-\sum_{j\in\mathcal{I}(i),\,j\neq i}\boldsymbol{d}_{ij}^L.$$

In practice, computing $\lambda_{\max}$ exactly is expensive since a one-dimensional Riemann problem needs to be solved for each pair $(i,j), i\neq j$. Fortunately, an efficient-to-compute close enough upper bound $\lambda^\#\geq\lambda_{\max}$ can be used instead. A fast algorithm to compute $\lambda^\#$ can be looked up in [30, 41].

We introduce the bar states

$$\overline{\mathbf{U}}_{ij}^n:=\frac{1}{2}(\mathbf{U}_i^n+\mathbf{U}_j^n)-\frac{\|\boldsymbol{c}_{ij}\|}{2\boldsymbol{d}_{ij}^L}(\mathbb{F}(\mathbf{U}_j^n)-\mathbb{F}(\mathbf{U}_i^n))\boldsymbol{n}_{ij},$$

each can be shown to be a Riemann average of the Riemann solution $\mathbf{U}(\mathbf{U}_i^n,\mathbf{U}_j^n,\boldsymbol{n}_{ij})$. Therefore, the bar states $\overline{\mathbf{U}}_{ij}^n$ are also in $\mathcal{A}$. The equation (4.5) can be rewritten as a convex combination of $\mathbf{U}_i^n$ and $\overline{\mathbf{U}}_{ij}^n$,

$$\mathbf{U}_i^{L,n+1}=\left(1-\sum_{j\in\mathcal{I}(i),j\neq i}\frac{2\tau\boldsymbol{d}_{ij}^{L,n}}{m_i}\right)\mathbf{U}_i^n+\left(\sum_{j\in\mathcal{I}(i),j\neq i}\frac{2\tau\boldsymbol{d}_{ij}^{L,n}}{m_i}\right)\bar{\mathbf{U}}_{ij}^n,$$

if the time step size follows the CFL condition,

$$\tau\leq\min_i\left(\frac{m_i}{-2\boldsymbol{d}_{ii}^{L,n}}\right).$$

Therefore, the low-order solution $\mathbf{U}_i^{L,n+1}$ is also in $\mathcal{A}$.

A high-order scheme is formulated similarly to the low-order scheme, but the coefficients $\boldsymbol{d}_{ij}$ are calculated by a high-order viscosity method, for example by EV or RV. The high-order solution $\mathbf{U}_i^{H,n+1}$ is obtained by solving

$$\sum_{j\in\mathcal{I}(i)}\left(m_{ij}\frac{\mathbf{U}_i^{H,n+1}-\mathbf{U}_i^n}{\tau}\right)+\sum_{j\in\mathcal{I}(i)}\left(\mathbb{F}(\mathbf{U}_j^n)\boldsymbol{c}_{ij}-\boldsymbol{d}_{ij}^H(\mathbf{U}_j^n-\mathbf{U}_i^n)\right)=\mathbf{0}. \tag{4.6}$$

The full mass matrix m_{ij} is used to reduce dispersion errors. The high-order graph viscosities $\boldsymbol{d}_{ij}^H$ must follow the symmetry and conservation constraints, $\boldsymbol{d}_{ij}^H = \boldsymbol{d}_{ji}^H$, $\boldsymbol{d}_{ii}^H = -\sum_{j\in\mathcal{I}(i),j\neq i} \boldsymbol{d}_{ij}^H$.

The low-order solution $\mathbf{U}_h^L$ is in the invariant domain but first-order accurate at best. The high-order solution $\mathbf{U}_h^H$ has second-order smooth convergence but is not guaranteed to be in the invariant domain. Therefore, a limiting procedure, illustrated in Figure 4.2, is necessary to achieve the best of both: second-order accuracy for smooth solutions while guaranteeing the preservation of the invariant domain. Because $\mathcal{A}$ is convex, the existence and uniqueness of $\mathbf{U}_h^{n+1}$ via such a limiter is straightforward. Now we rewrite the low-order and high-order schemes to design the convex limiter

$$m_i(\mathbf{U}_i^{L,n+1} - \mathbf{U}_i^n) + \sum_{j\in\mathcal{I}(i)} \boldsymbol{F}_{ij}^L = \mathbf{0},$$

and

$$m_i(\mathbf{U}_i^{H,n+1} - \mathbf{U}_i^n) + \sum_{j\in\mathcal{I}(i)} \boldsymbol{F}_{ij}^H = \mathbf{0},$$

where

$$\begin{aligned}
\boldsymbol{F}_{ij}^L &= \tau(\mathbb{F}(\mathbf{U}_j^n) + \mathbb{F}(\mathbf{U}_i^n))\boldsymbol{c}_{ij} - \tau\boldsymbol{d}_{ij}^L(\mathbf{U}_j^n - \mathbf{U}_i^n),\\
\boldsymbol{F}_{ij}^H &= \tau(\mathbb{F}(\mathbf{U}_j^n) + \mathbb{F}(\mathbf{U}_i^n))\boldsymbol{c}_{ij} - \tau\boldsymbol{d}_{ij}^H(\mathbf{U}_j^n - \mathbf{U}_i^n),\\
&\quad + (m_{ij} - \delta_{ij}m_i)(\mathbf{U}_j^{H,n+1} - \mathbf{U}_j^n - \mathbf{U}_i^{H,n+1} + \mathbf{U}_i^n).
\end{aligned}$$

By defining $\boldsymbol{A}_{ij} := \boldsymbol{F}_{ij}^L - \boldsymbol{F}_{ij}^H$, the limited solution $\mathbf{U}_i^{n+1}$ can be written in a convenient formula,

$$\mathbf{U}_i^{n+1} = \mathbf{U}_i^{L,n+1} + \frac{1}{m_i}\sum_{j\in\mathcal{I}(i)} \ell_{ij}\boldsymbol{A}_{ij},$$

where the limiters ℓ_{ij} are in $[0,1]$. To optimize accuracy, we want to find the largest ℓ_{ij} such that $\mathbf{U}_h^{n+1}$ is still in $\mathcal{A}$. When $\ell_{ij} \equiv 0\ \forall i,j$, $\mathbf{U}_h^{n+1}$ becomes the first-order solution $\mathbf{U}_h^{L,n+1}$. On the other hand, if $\mathbf{U}_h^{H,n+1}$ is already in $\mathcal{A}$, then we can set $\ell_{ij} \equiv 1$. Finding the optimal ℓ_{ij} can be done via a line search. The interested readers are referred to [38, 62] for the details on implementation.

We also note that the evolution of the discrete solution in the source system updates ensures pointwise preservation of density, internal energy, and specific entropy. Therefore, as long as the Euler solver guarantees invariant-domain preservation, the complete scheme is invariant-domain preserving.

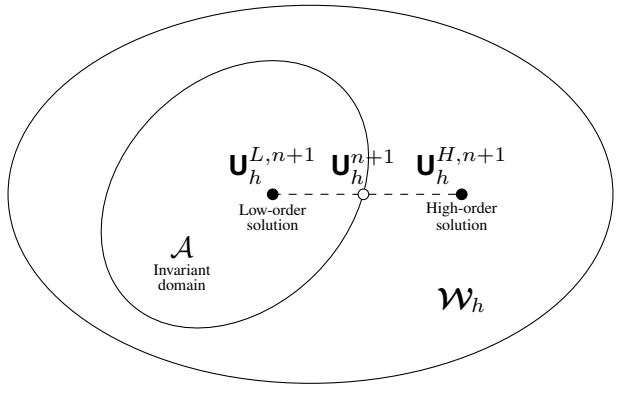

Figure 4.2. Illustration of the convex limiting technique. From the low-order solution $\boldsymbol{u}_h^{L,n+1} \in \mathcal{A}$ and the high-order solution $\boldsymbol{u}_h^{H,n+1}$, the limited solution $\boldsymbol{u}_h^{n+1}$ is computed via a line search.

4.3 Energy conservation and entropy dissipation

After the update procedure from time t^n to t^{n+1}, the total energy is conservative in the following sense,

$$\sum_{i\in\mathcal{N}_h} m_i\mathcal{E}_i^{n+1} + \frac{1}{2}\|\boldsymbol{B}_h^{n+1}\|_{L^2(\Omega)}^2 = \sum_{i\in\mathcal{N}_h}^{N} m_i\mathcal{E}_i^{n} + \frac{1}{2}\|\boldsymbol{B}_h^{n}\|_{L^2(\Omega)}^2.$$

Since the source-system discretization preserves pointwise values of specific entropy, entropy properties of the complete scheme are inherited from the Euler discretization. As a consequence of convex limiting, the discrete entropy is dissipative in the following sense,

$$\sum_{i\in\mathcal{N}_h} m_i S(\boldsymbol{u}_i^{n+1}) \leq \sum_{i\in\mathcal{N}_h} m_i S(\boldsymbol{u}_i^{n}),$$

where $S(\boldsymbol{u}_i) := -\rho_i s(\boldsymbol{u}_i)$ is the mathematical entropy.

4.4 Preservation of weak magnetic divergence

In this section we illustrate another advantage of utilizing the non-divergence formulation (4.1). By using an appropriate space to seek the magnetic field solution, we can guarantee zero divergence of $\boldsymbol{B}_h$ in a weak sense.

We discuss the purposeful choice of the function space $\boldsymbol{\mathcal{H}}_h$ for the magnetic solution $\boldsymbol{B}_h$, associating with a test space $\mathcal{Q}_h^*$ to define the weak divergence. First, let us define two more abstract function spaces,

$$H(\text{curl},\Omega) := \{\varphi \in [L^2(\Omega)]^d | \nabla\times\varphi \in [L^2(\Omega)]^d\}$$

and

$$H(\mathrm{div},\Omega) := \{\varphi \in [L^2(\Omega)]^d | \nabla\cdot\varphi \in [L^2(\Omega)]^d\}.$$

Function spaces of electromagnetics often follow the L^2–de Rham complex [7]. In three spatial dimensions, the sequence has the form,

$$\begin{array}{ccccccc} H^1(\Omega) & \xrightarrow{\nabla} & H(\mathrm{curl},\Omega) & \xrightarrow{\nabla\times} & H(\mathrm{div},\Omega) & \xrightarrow{\nabla\cdot} & L^2(\Omega) \\ \cup & & \cup & & & & \\ \mathcal{Q}_h^* & \xrightarrow{\nabla} & \boldsymbol{\mathcal{H}}_h & & & & \end{array}$$

where in the first row, an application of the two consecutive differential operators maps every function to zero, for example, $\nabla\times\nabla\varphi = 0$ for any $\varphi \in H^1(\Omega)$. The second row contains finite element subspaces chosen such that they follow the rule of the first row. To be more precise, we require that $\mathcal{Q}_h^* \subset H^1(\Omega), \boldsymbol{\mathcal{H}}_h \subset H(\mathrm{curl},\Omega)$ such that taking any $\varphi \in \mathcal{Q}_h^*$, we have $\nabla\varphi \in \boldsymbol{\mathcal{H}}_h$, and as a consequence $\nabla\times\nabla\varphi = 0$. For example, in Paper V, $\boldsymbol{\mathcal{H}}_h$ is chosen to be the rotated BDM_1 elements, also known as Nédélec second kind elements, see [8, 49], and $\mathcal{Q}_h^*$ is chosen to be the space of continuous piecewise quadratic functions.

Now we show that the weak divergence is indeed preserved. Notice that $\boldsymbol{B}_h$ and the test function $\nabla\varphi$ where $\varphi \in \mathcal{Q}_h^*$ are in the same space $\boldsymbol{\mathcal{H}}_h$. Multiplying the induction equation in (4.4) with $\nabla\varphi$, we have

$$\int_\Omega (\boldsymbol{B}_h^{n+1} - \boldsymbol{B}_h^n)\cdot\nabla\varphi \,\mathrm{d}\boldsymbol{x} = \tau \int_\Omega (\boldsymbol{B}_h^{n+\frac{1}{2}} \times (\nabla\times\nabla\varphi))\cdot\boldsymbol{u}_h^{n+\frac{1}{2}} \,\mathrm{d}\boldsymbol{x}.$$

Because $\nabla\times\nabla\varphi = 0$ for all $\varphi \in \mathcal{Q}_h^*$, the equality is equivalent to

$$\int_\Omega \boldsymbol{B}_h^{n+1}\cdot\nabla\varphi \,\mathrm{d}\boldsymbol{x} = \int_\Omega \boldsymbol{B}_h^{n}\cdot\nabla\varphi \,\mathrm{d}\boldsymbol{x},$$

for all $\varphi \in \mathcal{Q}_h^*$, which means that the divergence in a weak sense is preserved from time step n to $n+1$. If the initial solution satisfies zero weak divergence, then the weak divergence remains zero over time.

5. Summary of papers

Papers I-V are briefly summarized in this section. The author of this thesis states his contribution to each of the papers.

5.1 Paper I

This paper proposes a robust high-order shock-capturing technique for the ideal MHD equations. Continuous Lagrange finite elements are used for spatial discretization and an explicit fourth-order Runge-Kutta scheme is used for temporal discretization. Based on the PDE residual, the stabilization term adds enough viscosity to precise locations of discontinuities to stabilize them. An advantage of this stabilization is that it does not lower the high-order accuracy of the base unstabilized scheme on smooth solutions. We demonstrate the efficacy of different methods for magnetic divergence cleaning such as projection method and generalized Lagrange multiplier. Several popular MHD benchmarks in the presence of discontinuities in one, two, and three spatial dimensions are tested. Results show agreement with the existing schemes in the literature, stability is achieved and the discontinuities are finely resolved.

Contribution: The author of this thesis developed ideas and constructed the method in close collaboration with the second author. The author wrote the code, performed numerical tests, and wrote parts of the paper.

5.2 Paper II

The main focus of this paper is the continuous analysis of the monolithic parabolic regularization defined in Section 3.1.1. The motivation is to advocate the use of the monolithic parabolic flux instead of the conventional resistive MHD model for numerical purposes. Several attractive properties are carefully proven in the paper: positivity of density and internal energy, minimum entropy principle, and compatibility with the generalized entropies. The analysis builds upon the works of [40] and [44] on the compressible Euler equations. To relate the continuous analysis to the numerical applications, an entropy viscosity finite element method is constructed where the viscous regularization is chosen as the monolithic parabolic flux. Several numerical examples are included, which show the numerical usability of the monolithic parabolic flux as a stabilization term and its advantages over the resistive MHD flux.

Contribution: The author of this thesis developed ideas and performed analysis in close collaboration with the second author. The author also wrote the code, performed numerical tests, and wrote parts of the paper.

5.3 Paper III

In this paper, we improve the formulation of the high-order residual viscosity in Paper I so that there is no appearance of tuning parameters. The motivation is that existing viscosity methods based on shock indicators, such as PDE residual or entropy residual, contain uncertain constants that may need to be tuned for different benchmarks. Our strategy introduces a sub-mesh of which mesh points coincide with the nodal points of the finite element space. This sub-mesh and its corresponding linear element space are then used to calculate the localized viscosity coefficient. For scalar equations, we prove that the proposed first-order scheme is invariant-domain preserving. Combining with the residual viscosity method, we demonstrate that this approach achieves high-order convergence for smooth solutions while effectively capturing discontinuities. The localization of artificial viscosity improves the robustness of high-order polynomials.

Contribution: The author of this thesis developed ideas and performed analysis in close collaboration with the second author. The author also wrote the code, performed numerical tests, and wrote parts of the paper.

5.4 Paper IV

This paper proposes a viscous regularization to the ideal MHD equations which is more general than the monolithic parabolic regularization in Paper II. The new viscous flux is an extension of the Guermond-Popov viscous flux [40] for compressible flows with an addition of the resistive MHD flux for the magnetic components. Many properties of the new flux, denoted GP, are the same as the monolithic flux: positivity of density and internal energy, minimum entropy principle, compatibility with the generalized entropies, Galilean and rotational invariance. Unlike the monolithic flux, the GP flux has a clear physical interpretation. It incorporates physical viscosity coefficients and magnetic resistivity. Another crucial physical property is the conservation of angular momentum, which is enjoyed by neither the monolithic flux nor the GP flux. In this article, we also provide an angular-momentum conserving variation of the GP flux. A further advancement from Paper II is that the analysis in this paper does not assume $\nabla \cdot \boldsymbol{B} = 0$. This makes the analysis more useful for numerical schemes because the divergence of numerical magnetic solutions is not usually zero.

Contribution: The author of this thesis developed ideas and performed analysis in close collaboration with the second and the third authors. The author also wrote the code, performed numerical tests, and wrote parts of the paper.

5.5 Paper V

The idea of this paper started from an observation of the viscous regularization developed in Paper II. We notice that the vanishing viscosity limits of the monolithic parabolic regularized MHD system, without the regularization of the magnetic field, are still compatible with the entropy inequalities and preserve positivity. This has led us to the construction of a novel invariant-domain preserving scheme with specific features: (i) The MHD system is solved in a non-divergence formulation where the magnetic contribution is treated as a source term; (ii) There is no viscosity stabilization in the induction equation. The solution procedure requires two system solvers: a compressible Euler solver and a source-system solver. By using the state-of-the-art invariant-domain preserving scheme first introduced in [39] for the compressible Euler solver, our MHD scheme provably conserves energy, respects the minimum entropy principle, and is positivity-preserving for density and internal energy. Using curl-conforming finite elements to discretize the magnetic field, the weak divergence is guaranteed to be exactly zero at the discrete level. Another distinctive feature of the new MHD scheme is that it requires no calculation of the magnetosonic waves or their estimations/bounds. The time step restriction is solely determined by the CFL condition of the Euler system. This feature allows the simulation of very low plasma-beta numbers when the magnetic strength is much more dominant than the hydrodynamic pressure. The numerical result shows robustness for even the most challenging MHD benchmarks.

Contribution: The author of this thesis developed ideas and performed analysis in close collaboration with the second and the third authors. The author also wrote the code, performed numerical tests, and wrote parts of the paper.

6. Conclusion and outlook

This thesis discusses the system of ideal MHD equations and several robust viscosity finite element schemes to solve it. In particular, at the PDE level, Papers II and IV have answered the fundamental question of viscous regularization for MHD. For practical computation, Papers I and III have developed highly accurate, efficient, and stable algorithms for MHD based on viscous regularization. In Paper V, the proposed numerical scheme simultaneously addresses many major challenges listed in the end of Chapter 2.

Papers I-V offer significant potential for future extensions. One may investigate the physical relevance of the GP flux in Paper IV as a model of magnetic resistivity and fluid viscosity. A natural development of Paper III is to design a convex limiter similarly to the framework of graph viscosity. A high-performance matrix-free implementation of Paper V would enable efficient computation in three dimensions. Developing a higher-order version of the scheme in Paper V is achievable, but it would necessitate further effort. It is also interesting to investigate other numerical methods such as DG, FV, and FD as a substitution for FE in the framework of Paper V. The idea of Paper V can be applied in other PDE applications which are related to MHD. An efficient computation of the maximum wave speed for MHD is still left unsolved and would be an intriguing task.

References

[1] Rémi Abgrall and Timothy Barth. Residual distribution schemes for conservation laws via adaptive quadrature. *SIAM J. Sci. Comput.*, 24(3):732–769, 2002.

[2] Remi Abgrall, Pierre Ramet, and Robin Huart. Numerical simulation of unsteady MHD flows and applications. *Magnetohydrodynamics c/c of Magnitnaia Gidrodinamika*, 45(2):225–232, 2009.

[3] Hannes Alfvén. Existence of electromagnetic-hydrodynamic waves. *Nature*, 150(3805):405–406, 1942.

[4] Hannes Alfvén and B Lindblad. Granulation, magneto-hydrodynamic waves, and the heating of the solar corona. *Monthly Notices of the Royal Astronomical Society*, 107(2):211–219, 1947.

[5] Martin Alnaes, Jan Blechta, Johan Hake, August Johansson, Benjamin Kehlet, Anders Logg, Chris Richardson, Johannes Ring, Marie E Rognes, and Garth N Wells. The FEniCS project version 1.5. *Archive of numerical software*, 3(100), 2015.

[6] T. D. Arber, A. W. Longbottom, C. L. Gerrard, and A. M. Milne. A staggered grid, Lagrangian-Eulerian remap code for 3-D MHD simulations. *J. Comput. Phys.*, 171(1):151–181, 2001.

[7] Douglas N. Arnold, Richard S. Falk, and Ragnar Winther. Differential complexes and stability of finite element methods. I. The de Rham complex. In *Compatible spatial discretizations*, volume 142 of *IMA Vol. Math. Appl.*, pages 24–46. Springer, New York, 2006.

[8] Douglas N Arnold and Anders Logg. Periodic table of the finite elements. *SIAM News*, 47(9):212, 2014.

[9] Dinshaw S. Balsara. Self-adjusting, positivity preserving high order schemes for hydrodynamics and magnetohydrodynamics. *J. Comput. Phys.*, 231(22):7504–7517, 2012.

[10] Dinshaw S. Balsara, Michael Dumbser, and Remi Abgrall. Multidimensional HLLC Riemann solver for unstructured meshes—with application to Euler and MHD flows. *J. Comput. Phys.*, 261:172–208, 2014.

[11] Dinshaw S. Balsara and Daniel Spicer. Maintaining pressure positivity in magnetohydrodynamic simulations. *J. Comput. Phys.*, 148(1):133–148, 1999.

[12] Melanie Basting and Dmitri Kuzmin. An FCT finite element scheme for ideal MHD equations in 1D and 2D. *J. Comput. Phys.*, 338:585–605, 2017.

[13] Marvin Bohm, Andrew R. Winters, Gregor J. Gassner, Dominik Derigs, Florian Hindenlang, and Joachim Saur. An entropy stable nodal discontinuous Galerkin method for the resistive MHD equations. Part I: Theory and numerical verification. *J. Comput. Phys.*, 422:108076, 35, 2020.

[14] J. U. Brackbill and D. C. Barnes. The effect of nonzero $\nabla \cdot \mathbf{B}$ on the numerical solution of the magnetohydrodynamic equations. *J. Comput. Phys.*, 35(3):426–430, 1980.

[15] Jeremiah U Brackbill. Numerical models for high beta magnetohydrodynamic flow. In *Computer Applications in Plasma Science and Engineering*, pages 422–457. Springer, 1987.
[16] Howard Brenner. Fluid mechanics revisited. *Physica A: Statistical Mechanics and its Applications*, 370(2):190–224, 2006.
[17] M. Brio and C. C. Wu. An upwind differencing scheme for the equations of ideal magnetohydrodynamics. *J. Comput. Phys.*, 75(2):400–422, 1988.
[18] Gui-Qiang Chen and Hermano Frid. Uniqueness and asymptotic stability of Riemann solutions for the compressible Euler equations. *Transactions of the American Mathematical Society*, 353(3):1103–1117, 2001.
[19] Yue Cheng, Fengyan Li, Jianxian Qiu, and Liwei Xu. Positivity-preserving DG and central DG methods for ideal MHD equations. *J. Comput. Phys.*, 238:255–280, 2013.
[20] Andrew J. Christlieb, Xiao Feng, David C. Seal, and Qi Tang. A high-order positivity-preserving single-stage single-step method for the ideal magnetohydrodynamic equations. *J. Comput. Phys.*, 316:218–242, 2016.
[21] Andrew J. Christlieb, Yuan Liu, Qi Tang, and Zhengfu Xu. Positivity-preserving finite difference weighted ENO schemes with constrained transport for ideal magnetohydrodynamic equations. *SIAM J. Sci. Comput.*, 37(4):A1825–A1845, 2015.
[22] Bennett Clayton, Jean-Luc Guermond, Matthias Maier, Bojan Popov, and Eric J. Tovar. Robust second-order approximation of the compressible Euler equations with an arbitrary equation of state. *J. Comput. Phys.*, 478:Paper No. 111926, 21, 2023.
[23] Arpad Csik, Herman Deconinck, and Stefaan Poedts. Monotone residual distribution schemes for the ideal magnetohydrodynamic equations on unstructured grids. *AIAA journal*, 39(8):1532–1541, 2001.
[24] Árpád Csík, Mario Ricchiuto, and Herman Deconinck. A conservative formulation of the multidimensional upwind residual distribution schemes for general nonlinear conservation laws. *J. Comput. Phys.*, 179(1):286–312, 2002.
[25] Wenlong Dai and Paul R. Woodward. A simple finite difference scheme for multidimensional magnetohydrodynamical equations. *J. Comput. Phys.*, 142(2):331–369, 1998.
[26] A. Dedner, F. Kemm, D. Kröner, C.-D. Munz, T. Schnitzer, and M. Wesenberg. Hyperbolic divergence cleaning for the MHD equations. *J. Comput. Phys.*, 175(2):645–673, 2002.
[27] Marc O. Delchini, Jean C. Ragusa, and Ray A. Berry. Entropy-based viscous regularization for the multi-dimensional Euler equations in low-Mach and transonic flows. *Comput. & Fluids*, 118:225–244, 2015.
[28] Dominik Derigs, Andrew R. Winters, Gregor J. Gassner, and Stefanie Walch. A novel high-order, entropy stable, 3D AMR MHD solver with guaranteed positive pressure. *J. Comput. Phys.*, 317:223–256, 2016.
[29] Dominik Derigs, Andrew R. Winters, Gregor J. Gassner, Stefanie Walch, and Marvin Bohm. Ideal GLM-MHD: about the entropy consistent nine-wave magnetic field divergence diminishing ideal magnetohydrodynamics equations. *J. Comput. Phys.*, 364:420–467, 2018.
[30] Alexandre Ern and Jean-Luc Guermond. *Finite Elements III: First-Order and*

Time-Dependent PDEs, volume 74. Springer Nature, 2021.
[31] Eduard Feireisl and Alexis Vasseur. New perspectives in fluid dynamics: Mathematical analysis of a model proposed by Howard Brenner. *New Directions in Mathematical Fluid Mechanics: The Alexander V. Kazhikhov Memorial Volume*, pages 153–179, 2010.
[32] Jeffrey P Freidberg. Ideal magnetohydrodynamic theory of magnetic fusion systems. *Reviews of Modern Physics*, 54(3):801, 1982.
[33] S Fromang, P Hennebelle, and R Teyssier. RAMSES-MHD: an AMR Godunov code for astrophysical applications. *SF2A-2005: Semaine de l'Astrophysique Francaise*, page 743, 2005.
[34] Pei Fu, Fengyan Li, and Yan Xu. Globally divergence-free discontinuous Galerkin methods for ideal magnetohydrodynamic equations. *J. Sci. Comput.*, 77(3):1621–1659, 2018.
[35] AH Glasser, CR Sovinec, RA Nebel, TA Gianakon, SJ Plimpton, MS Chu, DD Schnack, Nimrod Team, et al. The NIMROD code: a new approach to numerical plasma physics. *Plasma Physics and Controlled Fusion*, 41(3A):A747, 1999.
[36] Sergei K Godunov. Symmetric form of the equations of magnetohydrodynamics. *Numerical Methods for Mechanics of Continuum Medium*, 1:26–34, 1972.
[37] J. L. Guermond and R. Pasquetti. Entropy viscosity method for high-order approximations of conservation laws. In *Spectral and high order methods for partial differential equations*, volume 76 of *Lect. Notes Comput. Sci. Eng.*, pages 411–418. Springer, Heidelberg, 2011.
[38] Jean-Luc Guermond, Martin Kronbichler, Matthias Maier, Bojan Popov, and Ignacio Tomas. On the implementation of a robust and efficient finite element-based parallel solver for the compressible Navier-Stokes equations. *Comput. Methods Appl. Mech. Engrg.*, 389:Paper No. 114250, 26, 2022.
[39] Jean-Luc Guermond, Murtazo Nazarov, Bojan Popov, and Ignacio Tomas. Second-order invariant domain preserving approximation of the Euler equations using convex limiting. *SIAM J. Sci. Comput.*, 40(5):A3211–A3239, 2018.
[40] Jean-Luc Guermond and Bojan Popov. Viscous regularization of the Euler equations and entropy principles. *SIAM J. Appl. Math.*, 74(2):284–305, 2014.
[41] Jean-Luc Guermond and Bojan Popov. Fast estimation from above of the maximum wave speed in the Riemann problem for the Euler equations. *J. Comput. Phys.*, 321:908–926, 2016.
[42] Jean-Luc Guermond and Bojan Popov. Invariant domains and first-order continuous finite element approximation for hyperbolic systems. *SIAM J. Numer. Anal.*, 54(4):2466–2489, 2016.
[43] Jean-Luc Guermond, Bojan Popov, and Ignacio Tomas. Invariant domain preserving discretization-independent schemes and convex limiting for hyperbolic systems. *Comput. Methods Appl. Mech. Engrg.*, 347:143–175, 2019.
[44] Ami Harten, Peter D. Lax, C. David Levermore, and William J. Morokoff. Convex entropies and hyperbolicity for general Euler equations. *SIAM J. Numer. Anal.*, 35(6):2117–2127, 1998.
[45] Matthias Hoelzl, Guido TA Huijsmans, SJP Pamela, Marina Bécoulet, Eric Nardon, Francisco Javier Artola, Boniface Nkonga, Calin Vlad Atanasiu, Vinodh Bandaru, Ashish Bhole, et al. The JOREK non-linear extended MHD

code and applications to large-scale instabilities and their control in magnetically confined fusion plasmas. *Nuclear Fusion*, 61(6):065001, 2021.
[46] Mats Holmström, Shahab Fatemi, Yoshifumi Futaana, and Hans Nilsson. The interaction between the moon and the solar wind. *Earth, planets and space*, 64:237–245, 2012.
[47] Thomas J. R. Hughes, Guglielmo Scovazzi, and Tayfun E. Tezduyar. Stabilized methods for compressible flows. *J. Sci. Comput.*, 43(3):343–368, 2010.
[48] P. Janhunen. A positive conservative method for magnetohydrodynamics based on HLL and Roe methods. *J. Comput. Phys.*, 160(2):649–661, 2000.
[49] Robert C Kirby, Anders Logg, Marie E Rognes, and Andy R Terrel. Common and unusual finite elements. In *Automated Solution of Differential Equations by the Finite Element Method: The FEniCS Book*, pages 95–119. Springer, 2012.
[50] AL Kritcher, AB Zylstra, CR Weber, OA Hurricane, DA Callahan, DS Clark, L Divol, DE Hinkel, K Humbird, O Jones, et al. Design of the first fusion experiment to achieve target energy gain g> 1. *Physical Review E*, 109(2):025204, 2024.
[51] D. Kuzmin and S. Turek. Flux correction tools for finite elements. *J. Comput. Phys.*, 175(2):525–558, 2002.
[52] Dmitri Kuzmin and Nikita Klyushnev. Limiting and divergence cleaning for continuous finite element discretizations of the MHD equations. *J. Comput. Phys.*, 407:109230, 18, 2020.
[53] SH Lai and LH Lyu. Nonlinear evolution of the MHD Kelvin-Helmholtz instability in a compressible plasma. *Journal of Geophysical Research: Space Physics*, 111(A1), 2006.
[54] Peter D Lax. Hyperbolic systems of conservation laws ii. *Communications on pure and applied mathematics*, 10(4):537–566, 1957.
[55] Randall J LeVeque. *Finite volume methods for hyperbolic problems*, volume 31. Cambridge university press, 2002.
[56] Fengyan Li and Chi-Wang Shu. Locally divergence-free discontinuous Galerkin methods for MHD equations. *J. Sci. Comput.*, 22/23:413–442, 2005.
[57] Michael W Liemohn, RA Frahm, JD Winningham, Y Ma, S Barabash, R Lundin, JU Kozyra, AF Nagy, SM Bougher, James Bell, et al. Numerical interpretation of high-altitude photoelectron observations. *Icarus*, 182(2):383–395, 2006.
[58] Mengqing Liu, Man Zhang, Caixia Li, and Fang Shen. A new locally divergence-free WLS-ENO scheme based on the positivity-preserving finite volume method for ideal MHD equations. *J. Comput. Phys.*, 447:Paper No. 110694, 24, 2021.
[59] Lukas Lundgren and Ken Mattsson. An efficient finite difference method for the shallow water equations. *J. Comput. Phys.*, 422:109784, 28, 2020.
[60] Lukas Lundgren and Murtazo Nazarov. A high-order residual-based viscosity finite element method for incompressible variable density flow. *J. Comput. Phys.*, 497:Paper No. 112608, 23, 2024.
[61] Sibusiso Mabuza, John N. Shadid, Eric C. Cyr, Roger P. Pawlowski, and Dmitri Kuzmin. A linearity preserving nodal variation limiting algorithm for continuous Galerkin discretization of ideal MHD equations. *J. Comput. Phys.*, 410:109390, 28, 2020.

[62] Matthias Maier and Martin Kronbichler. Efficient parallel 3D computation of the compressible Euler equations with an invariant-domain preserving second-order finite-element scheme. *ACM Trans. Parallel Comput.*, 8(3):Art. 16, 30, 2021.
[63] Eckart Marsch, Hui Tian, Jian Sun, Werner Curdt, and Thomas Wiegelmann. Plasma flows guided by strong magnetic fields in the solar corona. *The Astrophysical Journal*, 685(2):1262, 2008.
[64] Xiong Meng and Jennifer K. Ryan. Discontinuous Galerkin methods for nonlinear scalar hyperbolic conservation laws: divided difference estimates and accuracy enhancement. *Numer. Math.*, 136(1):27–73, 2017.
[65] Andrea Mignone, Petros Tzeferacos, and Gianluigi Bodo. High-order conservative finite difference GLM-MHD schemes for cell-centered MHD. *J. Comput. Phys.*, 229(17):5896–5920, 2010.
[66] AB Mikhailovskii, JG Lominadze, AP Churikov, and VD Pustovitov. Progress in theory of instabilities in a rotating plasma. *Plasma physics reports*, 35:273–314, 2009.
[67] Murtazo Nazarov. Convergence of a residual based artificial viscosity finite element method. *Comput. Math. Appl.*, 65(4):616–626, 2013.
[68] Murtazo Nazarov and Johan Hoffman. Residual-based artificial viscosity for simulation of turbulent compressible flow using adaptive finite element methods. *Internat. J. Numer. Methods Fluids*, 71(3):339–357, 2013.
[69] Hans Christian Öttinger, Henning Struchtrup, and Mario Liu. Inconsistency of a dissipative contribution to the mass flux in hydrodynamics. *Physical Review E*, 80(5):056303, 2009.
[70] SJP Pamela, Ashish Bhole, GTA Huijsmans, Boniface Nkonga, Matthias Hoelzl, Isabel Krebs, Erika Strumberger, and JET Contributors. Extended full-MHD simulation of non-linear instabilities in tokamak plasmas. *Physics of Plasmas*, 27(10), 2020.
[71] Kenneth G Powell. An approximate Riemann solver for magnetohydrodynamics (that works in more than one dimension). Technical report, 1994.
[72] PH Rebut, D Boucher, DJ Gambier, BE Keen, and ML Watkins. The ITER challenge. *Fusion Engineering and Design*, 22(1-2):7–18, 1993.
[73] Andrés M. Rueda-Ramírez, Sebastian Hennemann, Florian J. Hindenlang, Andrew R. Winters, and Gregor J. Gassner. An entropy stable nodal discontinuous Galerkin method for the resistive MHD equations. Part II: Subcell finite volume shock capturing. *J. Comput. Phys.*, 444:Paper No. 110580, 48, 2021.
[74] Denis Serre. *Systems of Conservation Laws 2: Geometric Structures, Oscillations, and Initial-Boundary Value Problems*, volume 2. Cambridge University Press, 1999.
[75] Taras Siversky, Yuriy Voitenko, and Marcel Goossens. Shear flow instabilities in low-beta space plasmas. *Space science reviews*, 121:343–351, 2005.
[76] James M Stone and Thomas Gardiner. Nonlinear evolution of the magnetohydrodynamic rayleigh-taylor instability. *Physics of Fluids*, 19(9), 2007.
[77] James M Stone, Kengo Tomida, Christopher J White, and Kyle G Felker. The Athena++ adaptive mesh refinement framework: design and magnetohydrodynamic solvers. *The Astrophysical Journal Supplement Series*, 249(1):4, 2020.

[78] Magnus Svärd. A new Eulerian model for viscous and heat conducting compressible flows. *Phys. A*, 506:350–375, 2018.
[79] Magnus Svärd. Analysis of an alternative Navier-Stokes system: weak entropy solutions and a convergent numerical scheme. *Math. Models Methods Appl. Sci.*, 32(13):2601–2671, 2022.
[80] Kazuya Takahashi and Shoichi Yamada. Regular and non-regular solutions of the Riemann problem in ideal magnetohydrodynamics. *Journal of Plasma Physics*, 79(3):335–356, 2013.
[81] Kazuya Takahashi and Shoichi Yamada. Exact Riemann solver for ideal magnetohydrodynamics that can handle all types of intermediate shocks and switch-on/off waves. *Journal of Plasma Physics*, 80(2):255–287, 2014.
[82] AMM Todd, J Manickam, M Okabayashi, MS Chance, RC Grimm, JM Greene, and JL Johnson. Dependence of ideal-MHD kink and ballooning modes on plasma shape and profiles in tokamaks. *Nuclear Fusion*, 19(6):743, 1979.
[83] T Török, Bernhard Kliem, and VS Titov. Ideal kink instability of a magnetic loop equilibrium. *Astronomy & Astrophysics*, 413(3):L27–L30, 2004.
[84] Manuel Torrilhon. Exact solver and uniqueness conditions for Riemann problems of ideal magnetohydrodynamics. *SAM Research Report*, 2002, 2002.
[85] Manuel Torrilhon. Uniqueness conditions for Riemann problems of ideal magnetohydrodynamics. *Journal of plasma physics*, 69(3):253–276, 2003.
[86] Terrence S. Tricco and Daniel J. Price. Constrained hyperbolic divergence cleaning for smoothed particle magnetohydrodynamics. *J. Comput. Phys.*, 231(21):7214–7236, 2012.
[87] John Von Neumann and Robert D Richtmyer. A method for the numerical calculation of hydrodynamic shocks. *Journal of applied physics*, 21(3):232–237, 1950.
[88] K. Waagan. A positive MUSCL-Hancock scheme for ideal magnetohydrodynamics. *J. Comput. Phys.*, 228(23):8609–8626, 2009.
[89] Chi Wang, Xiao Cheng Guo, Zhong Peng, Bin Bin Tang, Tian Ran Sun, Wen Ya Li, and You Qiu Hu. Magnetohydrodynamics (MHD) numerical simulations on the interaction of the solar wind with the magnetosphere: A review. *Science China Earth Sciences*, 56:1141–1157, 2013.
[90] Andrew R. Winters and Gregor J. Gassner. Affordable, entropy conserving and entropy stable flux functions for the ideal MHD equations. *J. Comput. Phys.*, 304:72–108, 2016.
[91] Kailiang Wu. Positivity-preserving analysis of numerical schemes for ideal magnetohydrodynamics. *SIAM J. Numer. Anal.*, 56(4):2124–2147, 2018.
[92] Kailiang Wu, Haili Jiang, and Chi-Wang Shu. Provably positive central discontinuous Galerkin schemes via geometric quasilinearization for ideal MHD equations. *SIAM J. Numer. Anal.*, 61(1):250–285, 2023.
[93] Kailiang Wu and Chi-Wang Shu. A provably positive discontinuous Galerkin method for multidimensional ideal magnetohydrodynamics. *SIAM J. Sci. Comput.*, 40(5):B1302–B1329, 2018.
[94] Kailiang Wu and Chi-Wang Shu. Provably positive high-order schemes for ideal magnetohydrodynamics: analysis on general meshes. *Numer. Math.*, 142(4):995–1047, 2019.
[95] Kailiang Wu and Chi-Wang Shu. Provably physical-constraint-preserving

discontinuous Galerkin methods for multidimensional relativistic MHD equations. *Numer. Math.*, 148(3):699–741, 2021.

[96] Ke Xu, Zhenxun Gao, Zhansen Qian, and Chun-Hian Lee. Exact ideal magnetohydrodynamic Riemann solutions considering the strength of intermediate shocks. *Physics of Fluids*, 36(1), 2024.

[97] Sergey Yakovlev, Liwei Xu, and Fengyan Li. Locally divergence-free central discontinuous Galerkin methods for ideal MHD equations. *Journal of Computational Science*, 4(1-2):80–91, 2013.

[98] Yize Yu, Yan Jiang, and Mengping Zhang. Free-stream preserving finite difference schemes for ideal magnetohydrodynamics on curvilinear meshes. *J. Sci. Comput.*, 82(1):Paper No. 23, 26, 2020.

[99] Man Zhang, Xueshang Feng, Xiaojing Liu, and Liping Yang. A provably positive, divergence-free constrained transport scheme for the simulation of solar wind. *The Astrophysical Journal Supplement Series*, 257(2):32, 2021.

Acta Universitatis Upsaliensis

Digital Comprehensive Summaries of Uppsala Dissertations from the Faculty of Science and Technology 2414

Editor: The Dean of the Faculty of Science and Technology

A doctoral dissertation from the Faculty of Science and Technology, Uppsala University, is usually a summary of a number of papers. A few copies of the complete dissertation are kept at major Swedish research libraries, while the summary alone is distributed internationally through the series Digital Comprehensive Summaries of Uppsala Dissertations from the Faculty of Science and Technology. (Prior to January, 2005, the series was published under the title "Comprehensive Summaries of Uppsala Dissertations from the Faculty of Science and Technology".)

Distribution: publications.uu.se
urn:nbn:se:uu:diva-532130

ACTA UNIVERSITATIS
UPSALIENSIS
2024